Geomorphology 290 (2017) 39–57

Contents lists available at ScienceDirect

Geomorphology

journal homepage: www.elsevier.com/locate/geomorph

Rainfall thresholds for possible landslide occurrence in Italy

Silvia Peruccacci[a,*], Maria Teresa Brunetti[a], Stefano Luigi Gariano[a,b], Massimo Melillo[a], Mauro Rossi[a], Fausto Guzzetti[a]

[a] CNR IRPI, via Madonna Alta 126, 06128 Perugia, Italy
[b] Università degli Studi di Perugia, Dipartimento di Fisica e Geologia, via A. Pascoli, 06123 Perugia, Italy

ARTICLE INFO

Keywords:
Landslide catalogue
Rainfall threshold
Statistical analysis
Italy
Environmental conditions

ABSTRACT

The large physiographic variability and the abundance of landslide and rainfall data make Italy an ideal site to investigate variations in the rainfall conditions that can result in rainfall-induced landslides. We used landslide information obtained from multiple sources and rainfall data captured by 2228 rain gauges to build a catalogue of 2309 rainfall events with – mostly shallow – landslides in Italy between January 1996 and February 2014. For each rainfall event with landslides, we reconstructed the rainfall history that presumably caused the slope failure, and we determined the corresponding rainfall duration D (in hours) and cumulated event rainfall E (in mm). Adopting a power law threshold model, we determined cumulated event rainfall–rainfall duration (ED) thresholds, at 5% exceedance probability, and their uncertainty. We defined a new national threshold for Italy, and 26 regional thresholds for environmental subdivisions based on topography, lithology, land-use, land cover, climate, and meteorology, and we used the thresholds to study the variations of the rainfall conditions that can result in landslides in different environments, in Italy. We found that the national and the environmental thresholds cover a small part of the possible DE domain. The finding supports the use of empirical rainfall thresholds for landslide forecasting in Italy, but poses an empirical limitation to the possibility of defining thresholds for small geographical areas. We observed differences between some of the thresholds. With increasing mean annual precipitation (MAP), the thresholds become higher and steeper, indicating that more rainfall is needed to trigger landslides where the MAP is high than where it is low. This suggests that the landscape adjusts to the regional meteorological conditions. We also observed that the thresholds are higher for stronger rocks, and that forested areas require more rainfall than agricultural areas to initiate landslides. Finally, we observed that a 20% exceedance probability national threshold was capable of predicting all the rainfall-induced landslides with casualties between 1996 and 2014, and we suggest that this threshold can be used to forecast fatal rainfall-induced landslides in Italy. We expect the method proposed in this work to define and compare the thresholds to have an impact on the definition of new rainfall thresholds for possible landslide occurrence in Italy, and elsewhere.

1. Introduction

In Italy, landslides are widespread and frequent phenomena. Trigila et al. (2010), and more recently Trigila et al. (2015) have recognized more than half a million landslides in Italy, covering 22,176 km^2, approximately 9% of the hilly and mountainous terrain of the country. Salvati et al. (2014) have reported that in the 66-year period 1950–2015, 6047 persons were killed, went missing, or were injured by 661 fatal landslides in Italy. This corresponds to an average landslide mortality of 9 fatalities every 10 million people per year in the period. Most of the harmful landslides in Italy were triggered by intense or prolonged rainfall (Guzzetti et al., 1994; Guzzetti and Tonelli, 2004), which can result in single landslides, in multiple landslides in a small area (e.g., Marchi et al., 2002; Calcaterra et al., 2003; Guzzetti et al., 2004; Ardizzone et al., 2012; Peres and Cancelliere, 2014; Borrelli et al., 2015; Lagomarsino et al., 2015; Terranova et al., 2015; Giannecchini et al., 2016; Napolitano et al., 2016), or in large populations of landslides occurring in regions extending for thousands of square kilometres (e.g., Crosta, 1998; Aleotti, 2004; Cardinali et al., 2006; Martelloni et al., 2012; Rosi et al., 2012).

The large physiographic variability of Italy, combined with the abundance of landslide and rainfall information, make Italy an ideal case to investigate variations in the rainfall conditions that can result in rainfall-induced landslides, depending on topographic, geological, climatic, and meteorological conditions. In this work, we use empirical rainfall thresholds to represent the rainfall conditions that can result in

* Corresponding author.
E-mail address: silvia.peruccacci@irpi.cnr.it (S. Peruccacci).

http://dx.doi.org/10.1016/j.geomorph.2017.03.031
Received 10 January 2017; Received in revised form 21 March 2017; Accepted 27 March 2017
Available online 02 April 2017

rainfall-induced landslides in Italy, and we study the variations (or lack of variations) of the thresholds in different environmental settings.

The paper is organized as follows. After a description of the general settings of Italy (Section 2), we describe a unique catalogue of 2309 rainfall events with landslides (N_E) that have caused 2819 landslides (N_L) in Italy in the period 1996–2014, and the sources and method used for its compilation (Section 3). Next, we exploit the catalogue to define empirical rainfall thresholds for possible landslide occurrence in Italy, and in a number of different environmental subdivisions (Section 4). This is followed by a discussion of the obtained thresholds (Section 5), including a comparison with similar, published thresholds. We conclude (Section 6) summarizing the main lessons learnt.

2. Study area

Our study area encompasses the whole of Italy that extends in southern Europe for 301,336 km^2, from 6° to 19° E, and from 37° to 47° N. From a physiographic perspective, Italy is characterized by two main mountain ranges, the Alps to the north, stretching 1200 km from E to W and separating the Italian peninsula from central Europe; and the Apennines, a mountain and hilly range that extends for 1200 km from NW to SE forming the backbone of the Italian peninsula. The Po River and the Veneto plains separate the Alps from the Apennines (Fig. 1a). Surrounded by the Adriatic, Ionian, Tyrrhenian, and Ligurian Seas, the Italian peninsula is bounded by > 7000 km of coasts, with many islands, including Sicily and Sardinia, the two largest islands in the Mediterranean.

Sedimentary, metamorphic and igneous rocks, ranging from Paleozoic to Recent in age, crop out in Italy, covered by a variety of soils ranging from < 1 m to several meters in thickness. Located where the Eurasian Plate meets the African Plate, Italy is almost entirely seismically active, and has 14 volcanoes, four of which are active. Given its location in the Western Mediterranean Sea and the latitude range, climate varies largely in Italy. In the north, climate is typically cold and without dry seasons, and locally Alpine. Along the peninsula climate is temperate, with the length and the intensity of the dry summers increasing southward. Mean annual precipitation ranges from < 400 mm in Sicily and Sardinia, to > 2000 mm in the northern Apennines and the eastern Alps. The western part of the peninsula receives more rain than the eastern part, which is windier. Almost everywhere in Italy, November is the wettest and July the driest month (Desiato et al., 2014).

Landslides are abundant and widespread in Italy. A national landslide mapping project has recognized 528,903 landslides in Italy (Trigila et al., 2010, 2015). This corresponds to a density of about two landslides per square kilometres of hilly or mountain terrain, and in many areas landslides cover > 10% of the landscape. In Italy, the main natural trigger of landslides is rainfall, followed by rapid snowmelt, and earthquakes (Guzzetti, 2000; Guzzetti and Tonelli, 2004). Landslides are most frequent in January (14.4%), followed by November (13.7%), and October (12.9%) (Guzzetti and Tonelli, 2004), whereas landslides with direct human consequences are most abundant in November, and the majority of the landslide casualties was reported in October (Salvati et al., 2016).

3. Materials and methods

3.1. Catalogue of rainfall events with landslides

To build a catalogue of rainfall events with landslides N_E, in Italy, we used accurate landslide and rainfall information.

We obtained information on rainfall-induced, mostly shallow, landslides searching digital and printed newspapers, blogs, landslide databases, scientific journals, technical documents, landslide event reports, and fire fighter reports. The later proved particularly useful, as they provided accurate information on the exact or approximate time of occurrence of many landslides. A set of rules were established to decide if the information on a landslide could be used to construct the catalogue. Landslides were considered if: (i) rainfall was the sole, or the main trigger of the failure, and landslides caused e.g., by rapid snow melt or by rain-on-snow events were excluded, (ii) the location of the landslide was known with a sufficient geographical accuracy to allow for the selection of a rain gauge suited to reconstruct the landslide rainfall history, and (iii) the time of occurrence of the landslide was known with at least a daily accuracy. Given these strict requirements, about half of the landslide information originally collected from the various sources was not used to build the catalogue, and was discarded.

A total of 2819 rainfall-induced landslides N_L, were retained, and used to build the catalogue of rainfall events with landslides, N_E. The majority of the landslides (78.1%) were inventoried using information obtained from national, regional and local newspapers; and the fire fighter reports were the source of information for 550 landslides (19.5%). The proportion of information collected from the various sources varied in the different regions, depending on the type, availability and richness of the sources. The region with the largest number of landslides (N_L = 417) was Marche, central Italy, followed by Calabria (271) and Sicily (267), in southern Italy. The least number of landslides were reported in Molise (N_L = 2), central Italy. The individual rainfall-induced landslides were mapped as single points, using Google Earth™ (Fig. 1b). The 2819 point landslides correspond to an average density of 0.9×10^{-2} per km^{-2}. Landslides in the catalogue cover the period from January 1996 to February 2014, with the majority of the landslides between 2008 and 2011 (Fig. 2a).

Following Peruccacci et al. (2012), we attributed to each landslide a level of mapping accuracy P, in four classes: high, P_1 < 1 km^2; medium, 1 ≤ P_{10} < 10 km^2; low, 10 ≤ P_{100} < 100 km^2; and very low 100 ≤ P_{300} < 300 km^2. In the catalogue, the majority of the landslides (1497, 53.1%) are located with an accuracy of 1 km^2 (P_1), followed by 1095 (38.8%) landslides located with an accuracy of 10 km^2 (P_2) (Fig. 2b). To each landslide we also attributed a level of temporal accuracy T, in three classes. Level T_1 was used when the time (minute to hour) of the failure was known; level T_2 when the part of the day (a period of 3–5 h) was known (i.e., early or late morning, early or late afternoon, middle of the night); and level T_3 was given to landslides for which only the day of occurrence was known. For 1050 landslides (37.3%) in the catalogue the exact or the approximate time of failure (T_1) is known, and for 990 (35.1%) the part of the day (T_2) is known. For the remaining 779 landslides (27.6%) only the day of the landslide (T_3) is known (Fig. 2c).

Where available, information on the landslide type was also collected. This was not simple, because some of the sources (e.g., newspapers, fire fighter reports, blogs) often used imprecise language to describe the landslides. This has introduced uncertainty in the catalogue. We classified the landslides as debris flow (DF), mud-flow (MF), earth-flow (EF), rock fall (RF), and generic shallow landslide (SL). Most of the landslides in the catalogue (2006, 71.2%) are classified as SL (Fig. 2d), due to the lack of a detailed description of the landslide type in the information sources.

To reconstruct the rainfall history of each landslide, we used sub-hourly rainfall measurements obtained from a national network of 2228 rain gauges operated by Regional and Provincial governments, and by the Italian Civil Protection Department (Fig. 1c). Additional rainfall measurements were obtained from local and regional rain gauge networks. We based the selection of the rain gauge used to reconstruct the possible rainfall history that resulted in a landslide on three main criteria (Peruccacci et al., 2012), namely: (i) the topographic distance between the landslide and the rain gauge, (ii) the difference in elevation between the landslide and the rain gauge, and (iii) the local morphological setting. The last two points were particularly relevant requirements in areas with complex orography (e.g., the Alps).

In this work, we defined a rainfall event as a period, or a sequence of periods, of continuous rainfall separated from the preceding and the

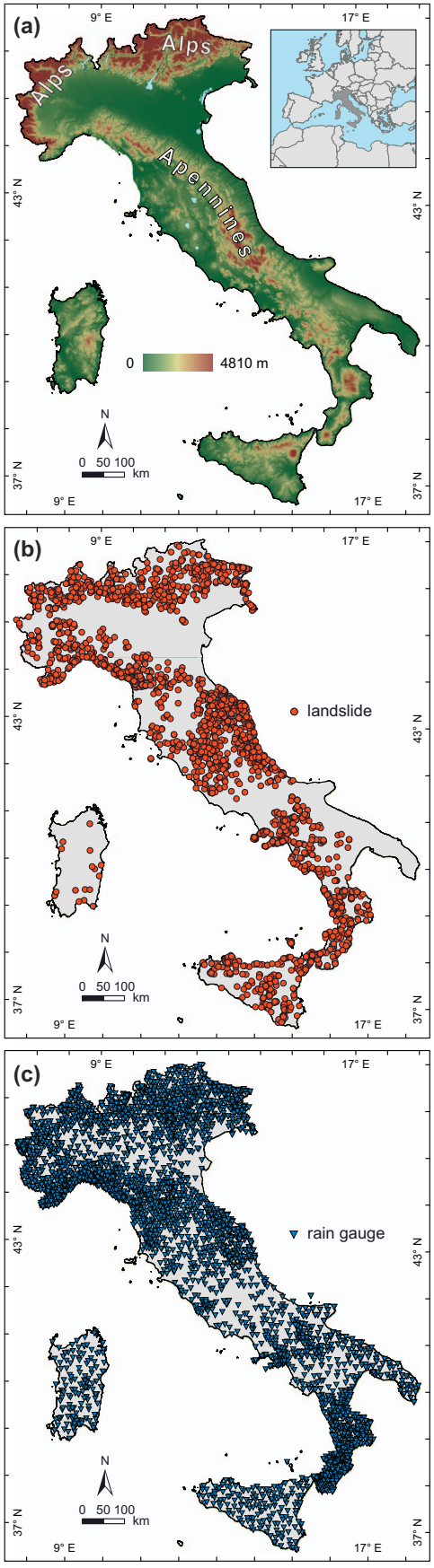

Fig. 1. (a) Map showing terrain elevation in Italy. Shades of colour show elevation obtained from the Shuttle Radar Topography Mission (SRTM) 90 m × 90 m DEM. (b) Location of 2819 rainfall-induced landslides (red dots) in Italy in the 19-year period from January 1996 to February 2014. (c) Location of 2228 rain gauges (blue triangles) available for this study. (For interpretation of the references to colour in this figure legend, the reader is referred to the web version of this article.)

(caption on next column)

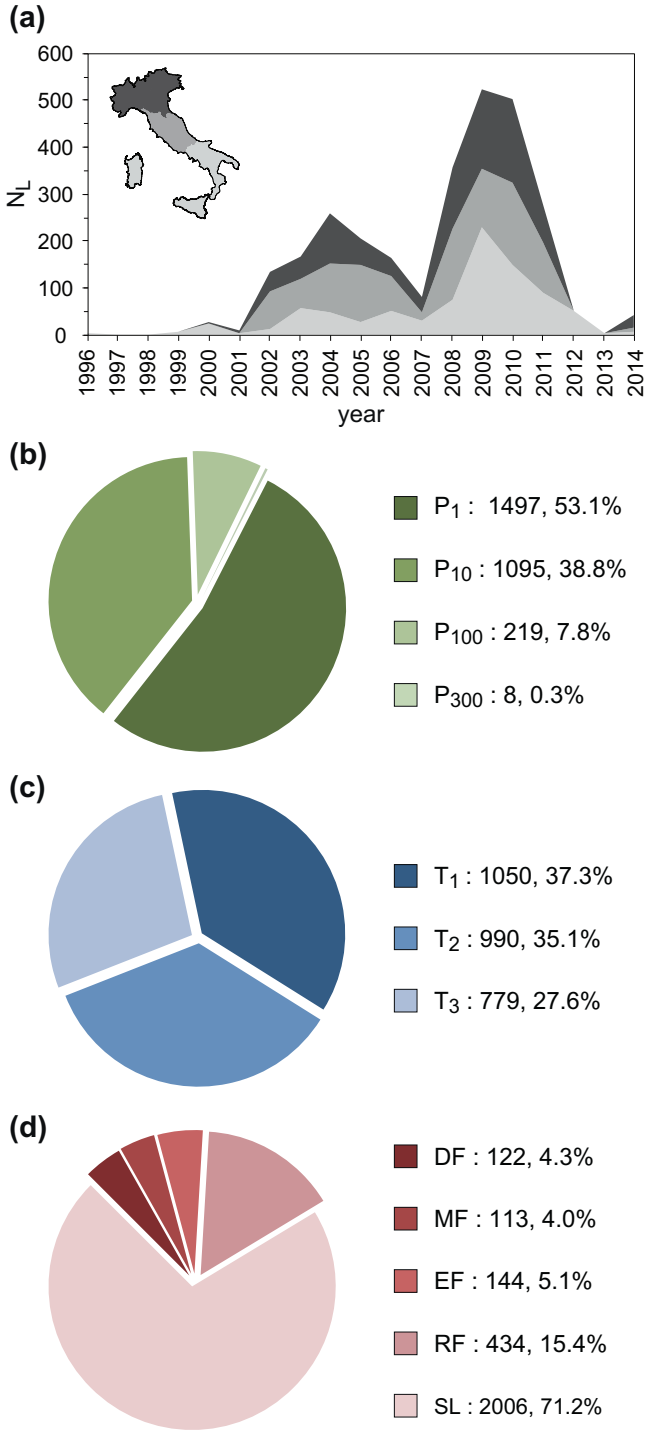

Fig. 2. (a) Stacked area chart shows, with three shades of grey, the number of landslides N_L, per year from January 1996 to February 2014, in northern, central, and southern Italy. Pie charts show (b) number and percentage of landslides with different levels of mapping accuracy (P_1, P_{10}, P_{100}, P_{300}), (c) number and percentage of landslides with different levels of temporal accuracy (T_1, T_2, T_3), and (d) number and percentage of landslides of different types. Legend: DF, debris flow; MF, mud flow; EF, earth flow; RF, rock fall; SL, generic shallow landslide.

following events by a dry period without rainfall (Brunetti et al., 2010; Peruccacci et al., 2012; Gariano et al., 2015a). We changed the length of the dry period depending on the seasonal conditions. Specifically, we used 48 h without rainfall for the dry season, and 96 h for the wet season. The length of the two seasonal periods (dry and wet) was selected as a function of the latitude, in three classes. In particular, in northern Italy the dry period was set from June to September and the wet period from October to May; in central Italy from May to September and from October to April; and in southern Italy from April to October and from November to March. Once a rainfall event was defined, we determined the duration D (in hour) of the rainfall that presumably triggered the landslide as the time interval (i.e., the period) between the start of the rainfall event and the time (known or inferred) of the landslide occurrence. Analogously, we determined the cumulated event rainfall E (in mm) for the rainfall duration D from the rainfall measurements captured by the selected rain gauge.

Overall, the catalogue lists 2309 rainfall events with landslides N_E, that have resulted in 2819 documented landslides N_L, in Italy, in the 19-year period from January 1996 to February 2014. $N_L > N_E$ because a single rainfall event may have triggered more than one landslide. For each rainfall event with landslides the catalogue lists the rainfall duration D (in hours), and the cumulated event rainfall E (in mm) that has resulted in one or more landslides. In the catalogue, rainfall events that resulted in landslides in Italy are in the range of duration $1\ h \le D \le 1212\ h$, and in the range of cumulated rainfall $4.2\ mm \le E \le 751.6\ mm$. Fig. 3a shows the distribution of the (D,E) points that caused one or more slope failures in Italy (grey dots) in linear coordinates and the marginal distributions of D and E (histograms) and their empirical cumulative distribution functions (red curves). Fig. 3b portrays the two-dimensional frequency density distribution (Kernel Density Estimation, KDE2d function, Bivand and Gebhardt, 2000) of the rainfall events in the orange shaded area of Fig. 3a. The 75% of rainfall conditions responsible for landslides are clustered in the range of duration and cumulated rainfall < 108 h and 137.0 mm, respectively. To the best of our knowledge, the catalogue is the single largest collection of information on rainfall events with landslides in Italy compiled specifically to determine rainfall thresholds for possible landslide occurrence.

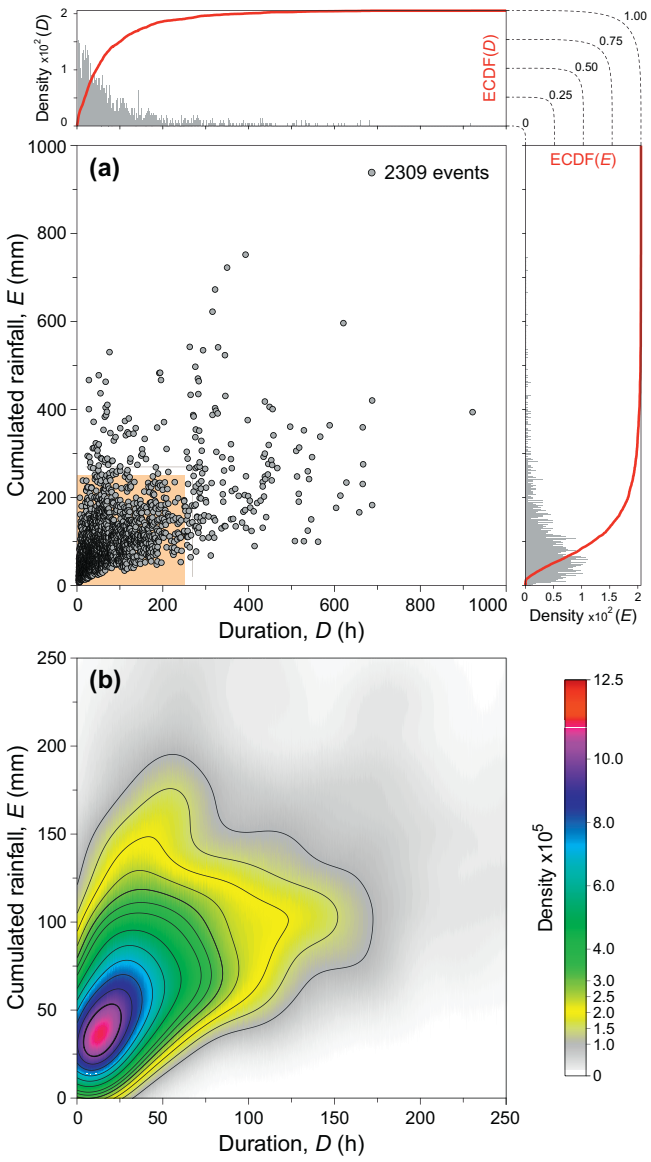

Fig. 3. (a) Rainfall duration D (h) vs. cumulated event rainfall E (mm) conditions that have resulted in landslides in Italy in the 19-year period from January 1996 to February 2014 (2309 grey dots). Data shown in linear coordinates. Orange area shows extent of chart portrayed in (b). Upper and right plots show marginal distributions of D and E (histograms) and their empirical cumulative distribution functions, ECDF (red lines). (b) Two-dimensional frequency density distribution of the (D,E) rainfall conditions for the orange area shown in (a). (For interpretation of the references to colour in this figure legend, the reader is referred to the web version of this article.)

3.2. Rainfall threshold model

To calculate objective and reproducible, cumulated event rainfall–rainfall duration, *ED* thresholds in Italy, we adopted the method proposed by Brunetti et al. (2010), and modified by Peruccacci et al. (2012). The method assumes that the threshold is represented by a power law curve, $E = (\alpha \pm \Delta\alpha) \times D^{(\gamma \pm \Delta\gamma)}$, where E is the cumulated (total) event rainfall (in mm), D is the duration of the rainfall event (in hours), α is a scaling parameter (the intercept), γ is the slope (the scaling exponent) of the power law curve, and $\Delta\alpha$ and $\Delta\gamma$ are the uncertainties associated to α and γ, respectively. The method allows calculating thresholds at several different exceedance probabilities. For this work, we selected 5% *ED* thresholds, that are expected to leave 5% of the empirical data points below the threshold line.

The uncertainties $\Delta\alpha$ and $\Delta\gamma$ measure the variation of the threshold around a central tendency line, and depend on multiple factors, but primarily on the number and the distribution of the empirical data points representing different rainfall conditions that have resulted in landslides in the *DE* domain. We found that there is a minimum number of rainfall events with landslides $N_E > 75$ above which the mean values of the parameters α and γ of a generic threshold remain stable i.e., $\left|\frac{\alpha_{N_E} - \alpha_n}{\alpha_{N_E}}\right| \le 2\%$ and $\left|\frac{\gamma_{N_E} - \gamma_n}{\gamma_{N_E}}\right| < 1\%$, where n is the number of the rainfall conditions responsible for landslides used to calculate the threshold ($n = 75, \ldots, N_E$). This minimum number depends chiefly on the distribution of the empirical data points in the *DE* domain. However, regardless of the distribution, for $N_E > 75$ the central tendency line representing the threshold remains stable, and only the uncertainty around the threshold decreases. For a definition of more reliable thresholds, and to reduce the uncertainty $\Delta\alpha$ and $\Delta\gamma$, in this work we define thresholds only for $N_E > 100$ (Table 1).

3.3. Environmental information

In addition to the landslide and the rainfall information presented before, we used small-scale environmental information obtained from different sources, including: (i) the map showing topographic subdivisions of Italy into eight provinces and 30 sub-provinces proposed by Guzzetti and Reichenbach (1994), at 1:1,200,000 scale, (ii) the Geological Map of Italy published by the Italian Istituto Superiore per la Protezione e la Ricerca Ambientale (ISPRA), at 1:500,000 scale, that shows 129 geological units, (iii) the pedological map of Italy published by Costantini et al. (2012), at 1:1,000,000 scale, showing 10 soil

Table 1
Rainfall *ED* thresholds for the possible initiation of landslides in Italy. Area shows the planimetric area (in km^2) of each region, computed in a GIS. N_L, number of landslides in the period from January 1996 to February 2014. N_E, number of rainfall events with landslides in the same period. *D*, rainfall duration (in hours). *E*, cumulated event rainfall (in mm). Threshold column lists the equations for the 5% *ED* power law threshold model lines, computed for regions where $N_E \geq 100$. Label, label of the new thresholds defined in this work.

Code	Region	Area km^2	N_L #	N_E #	*D* (h)			*E* (mm)			Threshold	Label
					min	mean	max	min	mean	max		
IT	Italy	301,336	2819	2309	1	84	1212	6.4	106.8	751.6	$E = 7.7 \pm 0.3 \times D^{(0.39 \pm 0.009)}$	$T_{5,IT}$
Topographic provinces												
P1	Alpine mountain system	51,665	616	546	1	89	684	6.4	127.6	751.6	$E = 6.3 \pm 0.4 \times D^{(0.47 \pm 0.02)}$	$T_{5,P1}$
P2	North Italian plain	47,513	49	42	1	83	282	26.5	128.1	243.8		
P3	Alpine-Apennine transition zone	6372	100	89	3	68	180	27.4	115.3	311.6		
P4	Apennine mountain system	81,153	1123	891	1	81	918	7.0	108.8	542,0	$E = 8.6 \pm 0.5 \times D^{(0.36 \pm 0.01)}$	$T_{5,P4}$
P5	Tyrrhenian borderland	38,246	316	275	1	130	1212	11.0	103.3	457.2	$E = 9.3 \pm 0.9 \times D^{(0.34 \pm 0.02)}$	$T_{5,P5}$
P6	Adriatic borderland	30,961	351	260	1	63	663	7.1	78.2	404.3	$E = 7.6 \pm 0.7 \times D^{(0.38 \pm 0.01)}$	$T_{5,P6}$
P7	Sicily	24,233	178	156	1	54	252	11.3	69.8	466.6	$E = 9.9 \pm 1.3 \times D^{(0.30 \pm 0.03)}$	$T_{5,P7}$
P8	Sardinia	21,193	17	17	12	88	434	16.7	88.2	247.3		
Lithological complexe												
AD	Alluvial deposit	73,631	152	142	1	77	450	7.2	96.4	464.0	$E = 9.8 \pm 0.5 \times D^{(0.34 \pm 0.03)}$	$T_{5,AD}$
CC	Carbonate rock complex	54,616	406	377	1	76	544	8.4	107.5	622.0	$E = 7.3 \pm 0.6 \times D^{(0.41 \pm 0.02)}$	$T_{5,CC}$
MC	Metamorphic rock	25,144	196	177	1	105	684	10.8	146.5	722.2	$E = 5.5 \pm 0.7 \times D^{(0.51 \pm 0.03)}$	$T_{5,MC}$
PO	Post-orogenic sediment	48,005	498	410	1	78	662	7.6	91.5	542.0	$E = 8.2 \pm 0.7 \times D^{(0.35 \pm 0.02)}$	$T_{5,PO}$
TC	Terrigenous complex	65,006	668	556	1	94	1212	9.2	113.2	751.6	$E = 9.0 \pm 0.8 \times D^{(0.37 \pm 0.02)}$	$T_{5,TC}$
VD	Volcanic deposit	17,154	133	117	2	92	1176	12.8	103.0	596.0	$E = 8.6 \pm 1.3 \times D^{(0.38 \pm 0.03)}$	$T_{5,VD}$
IR	Igneous rock	9847	47	41	1	52	254	20.4	136.4	477.6		
OR	Ophiolite rock	3376	13	13	1	81	355	16.0	84.7	264.7		
CH	Chaotic complex	2791	7	7	3	61	132	47.2	87.4	165.1		
GL	Glacier and lake	1097	0	0	–	–	–	–	–	–		
Pedological regions												
A	Soil of the Alps and the Prealps	50,119	598	534	1	88	684	6.4	129.2	751.6	$E = 6.4 \pm 0.4 \times D^{(0.47 \pm 0.02)}$	$T_{5,A}$
B	Soil of the Apennines with temperate climate	35,107	377	316	1	128	1212	8.0	115.7	496.9	$E = 8.3 \pm 0.9 \times D^{(0.38 \pm 0.02)}$	$T_{5,B}$
C	Soil of the hills of northern Italy	10,834	138	115	1	84	662	19.8	104.1	359.2	$E = 14.8 \pm 3.2 \times D^{(0.26 \pm 0.05)}$	$T_{5,C}$
D	Soil of the Po plain and related hills	47,754	39	34	4	82	226	25.8	128.6	348.0		
E	Soil of the central and southern Apennines	29,799	339	244	1	73	600	12.8	113.7	482.5	$E = 7.6 \pm 1.0 \times D^{(0.39 \pm 0.03)}$	$T_{5,E}$
F	Soil of Sardinia and Sicily on magmatic and metamorphic rocks	13,104	10	10	16	104	252	54.5	107.5	303.6		
G	Soil of hills in central and S Italy	47,444	579	488	1	70	662	11.3	94.3	542.0	$E = 8.5 \pm 0.6 \times D^{(0.35 \pm 0.02)}$	$T_{5,G}$
H	Soil of hills of central and S Italy on volcanic deposits	15,846	108	91	2	68	434	12.8	93.0	466.6		
I	Soil of hills and marine terraces of S Italy on calcareous sediments	17,380	75	67	2	61	182	11.4	68.5	139.7		
L	Soil of plains and low hills in central and southern Italy	26,827	89	78	1	90	1008	13.2	93.7	436.2		
U	Urban areas and water bodies	7136	65	65	1	78	450	11.0	89.4	287.2		
CORINE Land Cover classes												
AA	Agricultural area	157,239	712	594	1	74	1008	7.0	88.7	541.1	$E = 8.9 \pm 0.6 \times D^{(0.35 \pm 0.02)}$	$T_{5,AA}$
AS	Artificial surface	14,879	65	*64*	1	78	450	7.1	101.6	284.6		
FA	Forested and semi-natural area	125,378	557	504	1	80	514	6.4	122.9	722.2	$E = 6.9 \pm 0.5 \times D^{(0.45 \pm 0.02)}$	$T_{5,FA}$
WL	Wetland	668	0	*0*	–	–	–	–	–	–		
WB	Water body	3172	0	*0*	–	–	–	–	–	–		
Koeppen-Geiger climate regions												
Cfa	Temperate climate without dry season and with hot summer	96,690	591	457	1	101	1212	7	114.2	596.0	$E = 7.8 \pm 0.7 \times D^{(0.41 \pm 0.02)}$	$T_{5,Cfa}$
Cfb	Temperate climate without dry season and with warm summer	12,223	135	121	1	91	514	8.4	113.1	523.2	$E = 8.1 \pm 1.1 \times D^{(0.42 \pm 0.03)}$	$T_{5,Cfb}$
Csa	Temperate climate with dry and hot summer	148,667	1658	1354	1	78	1176	8.0	97.9	542.0	$E = 8.6 \pm 0.4 \times D^{(0.35 \pm 0.01)}$	$T_{5,Csa}$
Dfb	Cold climate without dry season and with warm summer	26,818	398	271	1	84	442	6.4	142	751.6	$E = 5.7 \pm 0.6 \times D^{(0.50 \pm 0.03)}$	$T_{5,Dfb}$
Csb	Temperate climate with dry and warm summer	7017	47	*47*	3	66	441	13.8	87.9	274.0		
Dfc	Cold climate without dry season and with cold summer	5465	46	*42*	1	76	321	10.8	96.3	371.1		
ET	Polar climate with tundra	2071	8	*8*	3	57	268	8.5	64.2	248.7		
Dfa	Cold climate without dry season and with hot summer	231	0	*0*	–	–	–	–	–	–		
Bsk	Arid steppe cold climate	2104	0	*0*	–	–	–	–	–	–		
Mean annual precipitation regions												
VL	Very low, MAP $\leq$ 800 mm	89,277	406	345	1	56	542	7.2	73.2	466.6	$E = 8.1 \pm 0.8 \times D^{(0.34 \pm 0.02)}$	$T_{5,VL}$
LO	Low, 800 < MAP $\leq$ 1200 mm	146,091	1503	1197	1	89	1176	6.4	99.5	542.0	$E = 7.9 \pm 0.4 \times D^{(0.37 \pm 0.01)}$	$T_{5,LO}$
ME	Medium, 1200 < MAP $\leq$ 1600 mm	51,987	610	557	1	93	1212	8.4	123.6	751.6	$E = 8.7 \pm 0.8 \times D^{(0.41 \pm 0.02)}$	$T_{5,ME}$
HI	High, 1600 < MAP $\leq$ 2000 mm	13,271	240	210	1	75	544	11.0	139.7	470.0	$E = 8.9 \pm 1.3 \times D^{(0.43 \pm 0.03)}$	$T_{5,HI}$
VH	Very high, MAP > 2000 mm	2991	61	*52*	2	91	355	12.8	216.1	496.9		

regions, (iv) the land cover map published by the Coordination of Information on the Environment (CORINE) project in 2006, at 1:100,000 scale, showing five first-level land use categories, (v) the world map of the Köppen-Geiger climate classification published by Peel et al. (2007) based on 0.5° × 0.5° latitude/longitude gridded data, and (vi) the map showing mean annual precipitation in Italy published by Desiato et al. (2014), at an undefined scale. We followed the procedure adopted by Peruccacci et al. (2012) to attribute the individual landslide in the catalogue to a specific environmental subdivision. In particular, each landslide, mapped as a single point, was represented by a circle, with the area (*A*) of the circle dependent on the mapping accuracy (P_1, $A = 0.5$ km^2; P_{10}, $A = 5$ km^2; P_{100},

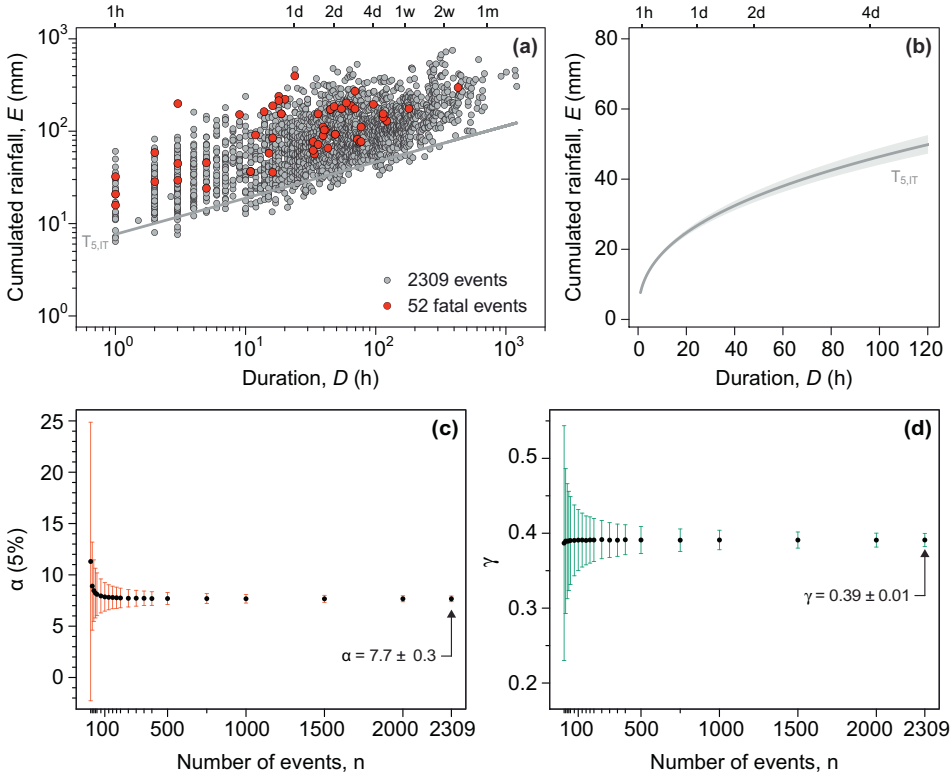

Fig. 4. (a) Rainfall duration D (h) vs. cumulated event rainfall E (mm) conditions that have resulted in landslides (N_E = 2309 grey and red dots) in Italy in the 19-period from January 1996 to February 2014, and corresponding 5% *ED* thresholds ($T_{5,IT}$, grey line). Red dots show sub-set of 52 N_E that have resulted in landslides with casualties in the same period. Data shown in log-log coordinates. (b) $T_{5,IT}$ threshold in the range 1 h ≤ D ≤ 120 h, in linear coordinates. Shaded area shows uncertainty around the threshold. (c) Variation in the power law threshold model parameter α (intercept), and associated uncertainty Δα (red bars), as a function of the number of events. (d) Variation in the power law threshold model parameter γ (scaling exponent), and associated uncertainty Δγ (green bars), as a function of the number of events. See text for explanation. (For interpretation of the references to colour in this figure legend, the reader is referred to the web version of this article.)

A = 50 km^2). Landslides belonging to P_{300} were excluded from the analysis. A given domain was attributed to each landslide where it covers at least 75% of the circle area. Details on the aggregation performed on the original maps, and the number of classes used to execute our analyses, are given in the next section, where we present the thresholds for different environmental subdivisions.

4. Rainfall thresholds

Using the catalogue of 2309 rainfall events with landslides presented before, and adopting the method proposed by Brunetti et al. (2010) and modified by Peruccacci et al. (2012), we determined objective cumulated event rainfall–rainfall duration (*ED*) thresholds, and their associated uncertainties, for Italy (Fig. 4) and for various geographical sub-sets, based on different small-scale environmental information, including topography (Fig. 5), lithology (Fig. 6), soil types (Fig. 7), land use (Fig. 8), climate (Fig. 9), and precipitation regimes (Fig. 10). Table 1 lists the main characteristics of the rainfall and landslide data used to define the thresholds, the ranges of rainfall duration D and cumulated event rainfall E, and the equations of the power law curves used to represent each threshold, with their associated uncertainty.

4.1. Threshold for Italy

Fig. 4a shows, in logarithmic coordinates, the distribution of the entire set of (*D,E*) rainfall conditions that have resulted in landslides in Italy (N_E = 2309 grey dots) in the 19-year considered period. In the log-log plot, the grey line is the 5% *ED* threshold for Italy, $T_{5,IT}$, with α = 7.7 ± 0.3 the intercept and γ = 0.39 ± 0.01 the slope of the threshold curve. The $T_{5,IT}$ threshold should leave 5% (N_E = 115) of the (*D,E*) empirical data points below the curve. In the chart, 101 points (4.4%) are below the threshold, most of which in the range 10 ≤ D ≤ 200 h, well approaching the number of data points expected below the threshold line. Fig. 4b portrays the same $T_{5,IT}$ threshold in linear coordinates, in the range 1 ≤ D ≤ 120 h. The shaded area around the threshold line shows the uncertainty associated to the threshold (Table 1), which is very small ($\Delta E/E$ < 0.08) for short rainfall durations (D ≤ 48 h), and increases for longer rainfall durations (e.g., for D = 480 h, $\Delta E/E$ = 0.12). We attribute the small uncertainty to the large number of empirical data points (Peruccacci et al., 2012; Vennari et al., 2014).

We analysed the relationship between the threshold parameters α and γ, their uncertainties Δα and Δγ, and the number of rainfall events with landslides N_E, for the selected 5% exceedance probability level. We determined the mean values of α and γ (black dots in Fig. 4c, d), and of Δα and Δγ (red vertical bars in Fig. 4c and green vertical bars in Fig. 4d, respectively) for an increasing number of events (n = 10, 20, 30, 40, 50, 75, 100, 125, 150, 175, 200, 250, 300, 350, 400, 500, 750, 1000, 1500, 2000, and 2309). We found that the mean value of α decreases gradually to α = 7.7 (e.g., for n = 10, α = 11.3, for n = 100, α = 7.8, and for n > 200, α = 7.7, Fig. 4c), whereas the mean value of γ does not vary significantly with the increasing number of the events, and converges rapidly to γ = 0.39 (Fig. 4d).

4.2. Thresholds for physiographic provinces

To investigate the role of the regional landscape morphology on rainfall thresholds, we used the topographic subdivision of Italy proposed by Guzzetti and Reichenbach (1994), who divided Italy into eight physiographic provinces reflecting different physical, geological and structural conditions (Fig. 5a). Adopting this topographic subdivi-

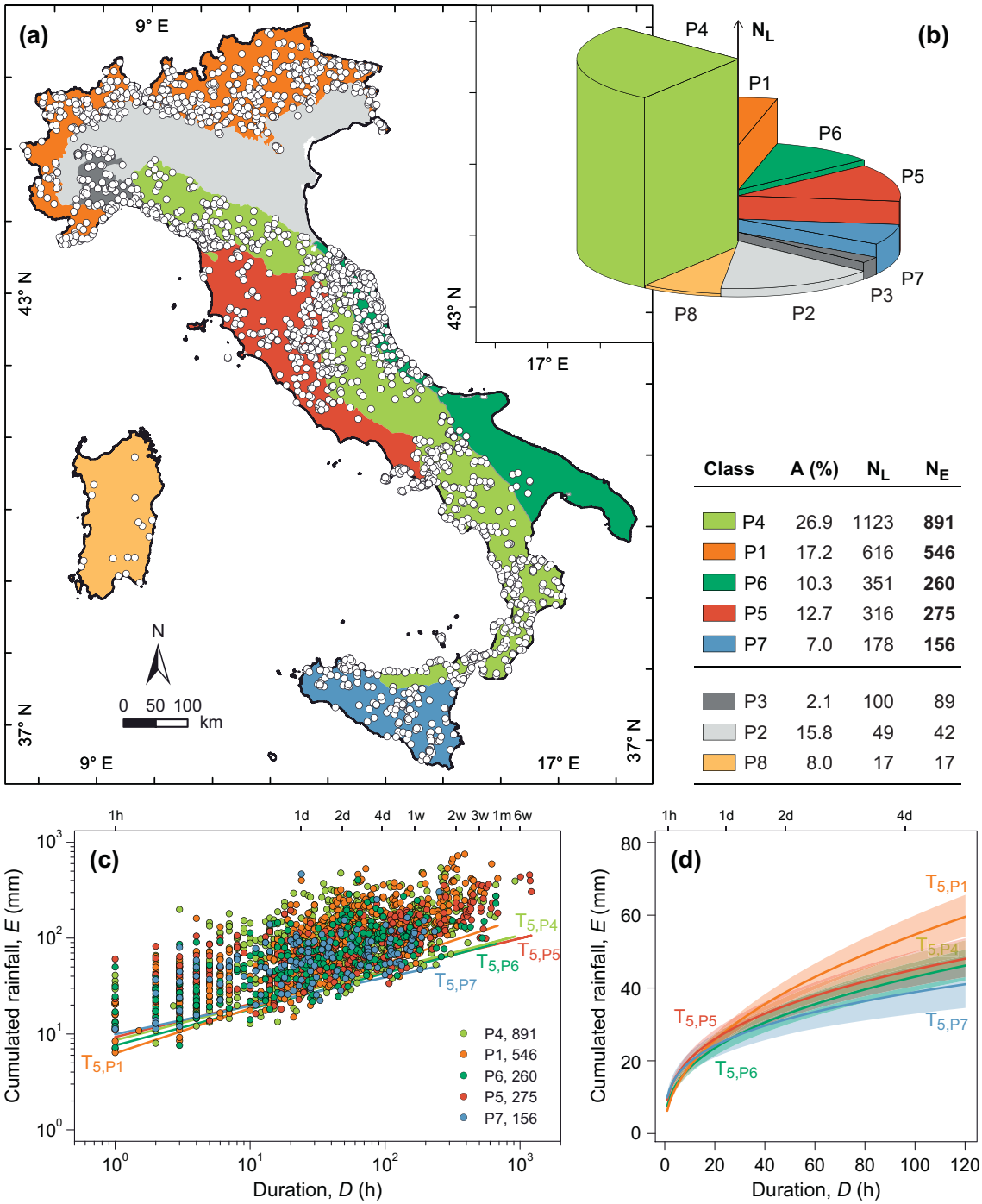

Fig. 5. (a) Map showing a subdivision of Italy into eight topographic provinces, modified after Guzzetti and Reichenbach (1994). Legend: P1, Alpine Mountain System; P2, North Italian Plain; P3, Alpine-Apennine Transition Zone; P4, Apennine Mountain System; P5, Tyrrhenian Borderland; P6, Adriatic Borderland; P7, Sicily; P8, Sardinia. (b) 3-Dimensional pie chart shows percentage of the topographic provinces (sector width) and number of rainfall-induced landslides (N_L, sector height). N_E is the number of landslide events in each topographic province. (c) Cumulated event rainfall E (mm) vs. rainfall duration D (h) conditions that resulted in landslides in P1 (orange dots), P4 (light green dots), P5 (red dots), P6 (green dots), and P7 (light blue dots). Coloured lines are corresponding 5% thresholds $T_{5,P1}$, $T_{5,P4}$, $T_{5,P5}$, $T_{5,P6}$, and $T_{5,P7}$. Data shown in log–log coordinates. (d) $T_{5,P1}$, $T_{5,P4}$, $T_{5,P5}$, $T_{5,P6}$, and $T_{5,P7}$ thresholds in the range 1 h ≤ D ≤ 120 h, with associated uncertainty portrayed by shaded areas, in linear coordinates. (For interpretation of the references to colour in this figure legend, the reader is referred to the web version of this article.)

sion, the Apennine mountain system (P4) has the largest area (80,903 km^2, 26.9%), followed by the Alpine mountain system (P1, 51,665 km^2, 17.2%), the North Italian plain (P2, 47,513 km^2, 15.8%), and the Tyrrhenian borderland (P5, 38,246 km^2, 12.7%). The Apennines (P4) have the largest number of landslides (N_L = 1123) and of rainfall events with landslides (N_E = 891), followed by the Alps (P1, N_L = 616, N_E = 546). The Adriatic borderland (P6) has more landslides (N_L = 351) than the Tyrrhenian borderland (P5, 316), but P5 has more rainfall events with landslides (N_E = 275) that P6 (260). Landslide density – i.e., the number of landslides per square kilometre – is largest in the Alps-Apennines transition zone (P3, 1.6 × 10^{-2} km^{-2}), followed by the Apennines mountain system (P4, 1.4 × 10^{-2} km^{-2}), and is lowest in Sardinia (P8, 0.7 × 10^{-3} km^{-2}).

Fig. 5c shows, in logarithmic coordinates, the distribution of the N_E = 2128 (D,E) rainfall conditions responsible for landslides in the five physiographic provinces that have N_E ≥ 100, including P4

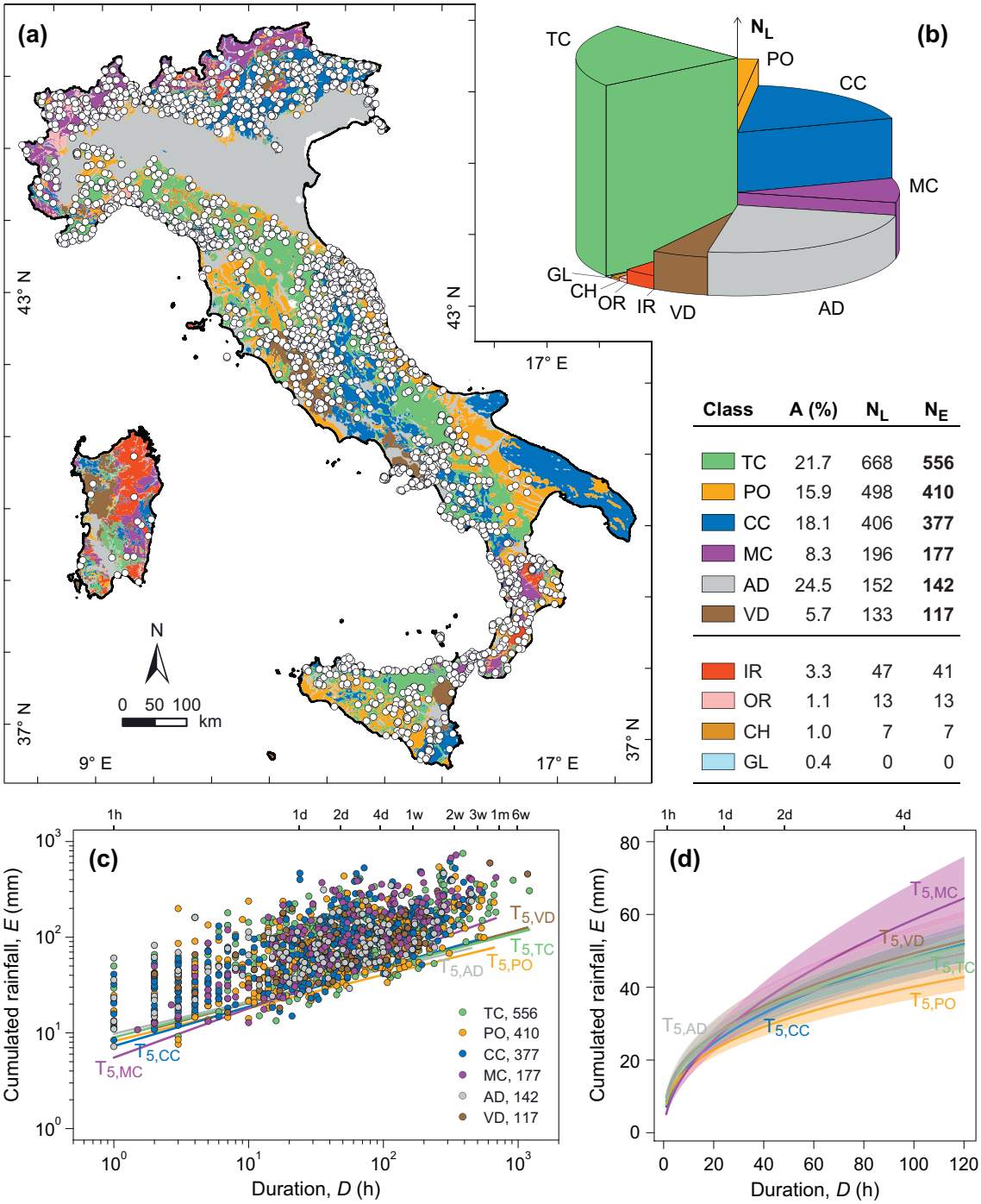

Fig. 6. (a) Map showing a subdivision of Italy in ten lithological complexes, modified from a map published by the Italian Istituto Superiore per la Protezione e la Ricerca Ambientale (ISPRA), at 1:500,000 scale. Legend: AD, alluvial deposit; TC, terrigenous complex (including flysch, turbidites with and without evaporite, marl and calcareous marl, layered sandstone and marl in various percentages with calcareous sandstone and argillite, argillite); CC, carbonate rocks complex; PO, post-orogenic sediments (including clay, marl, sand, and conglomerate); MC, metamorphic rock; VD, volcanic deposit; IR, igneous rocks; OR ophiolite rocks; CH, chaotic complex; GL, glaciers. White dots show location of rainfall-induced shallow landslides. (b) Pie chart shows percentage of extent of the lithological domains (A, sector width) and number of rainfall-induced landslides (N_L, sector height) in each lithological domain. (c) Cumulated event rainfall E (mm) vs. rainfall duration D (h) conditions that have resulted in landslides in the TC (green dots), PO (orange dots), CC (blue dots), MC (purple dots), AD (grey dots), and VD (brown dots) lithological domains. Coloured lines are corresponding 5% thresholds $T_{5,TC}$, $T_{5,PO}$, $T_{5,CC}$, $T_{5,MC}$, $T_{5,AD}$, and $T_{5,VD}$. Data shown in log–log coordinates. (d) $T_{5,TC}$, $T_{5,PO}$, $T_{5,CC}$, $T_{5,MC}$, $T_{5,AD}$, and $T_{5,VD}$ thresholds in the range 1 h ≤ D ≤ 120 h, with associated uncertainty portrayed by shaded areas, in linear coordinates. (For interpretation of the references to colour in this figure legend, the reader is referred to the web version of this article.)

(N_E = 891 light green dots), P1 (546 orange dots), P5 (275 red dots), P6 (260 green dots), and P7 (156 light blue dots), with the corresponding 5% *ED* thresholds, $T_{5,P4}$, $T_{5,P1}$, $T_{5,P5}$, $T_{5,P6}$, and $T_{5,P7}$ shown by the coloured lines (Table 1). The same thresholds are shown in Fig. 5d, in linear coordinates and in the range 1 ≤ D ≤ 120 h, with the shaded areas depicting the uncertainty associated to the thresholds. Inspection of Fig. 5c, d reveals that none of the five thresholds can be separated clearly, for the entire range of the considered rainfall durations. The threshold for the Alpine mountain system ($T_{5,P1}$) is steeper (γ = 0.47 ± 0.02) than the other thresholds, and the threshold for Sicily (P7) is the less steep threshold (γ = 0.47 ± 0.02). Considering the uncertainty, the other thresholds ($T_{5,P4}$, $T_{5,P5}$, and $T_{5,P6}$) are

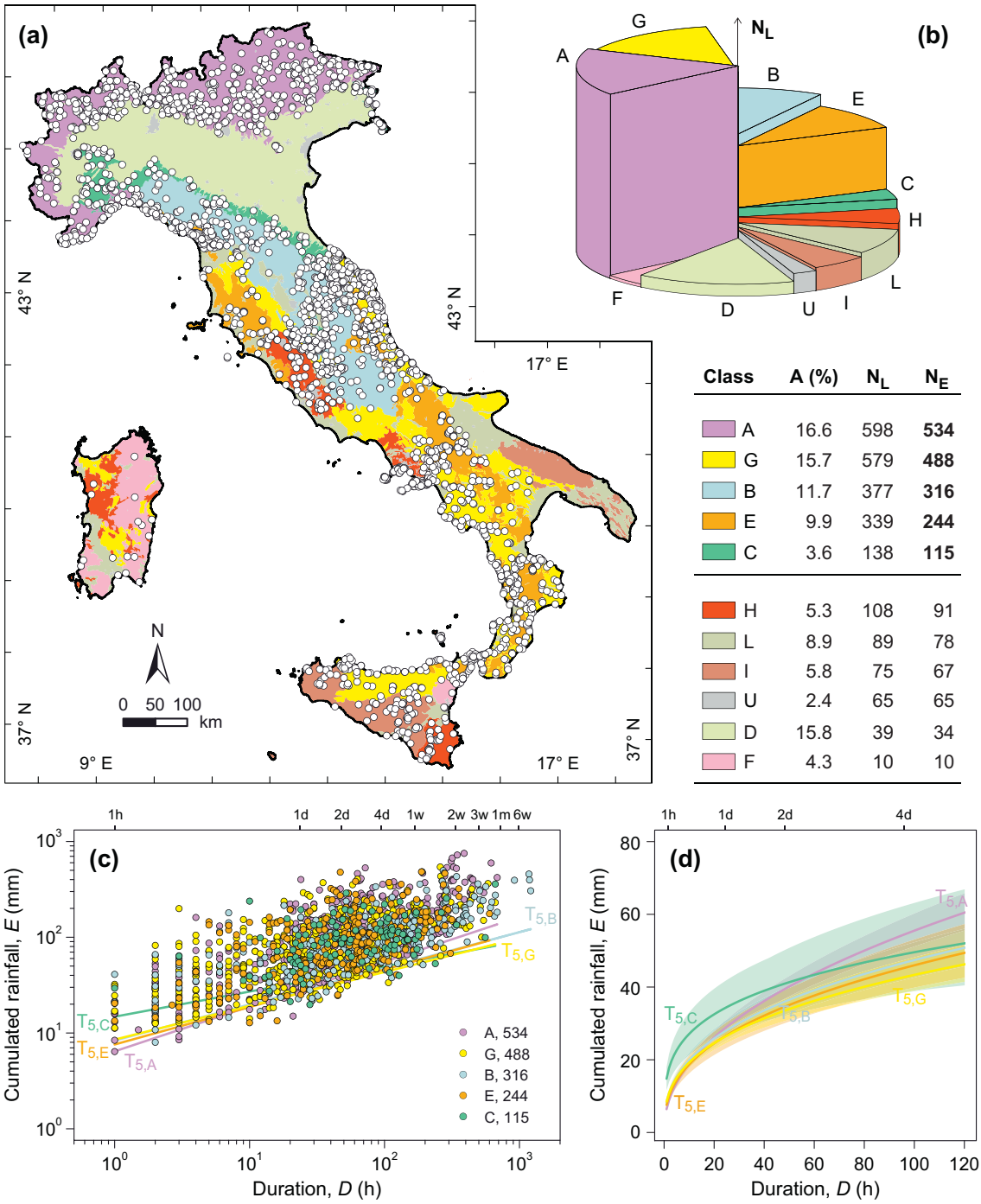

Fig. 7. (a) Map showing a subdivision of Italy in ten soil regions, urban areas and water bodies (U), modified after Costantini et al. (2012). Legend: A, soils of the Alps and Prealps; B, soils of the Apennines with temperate climate; C, soils of the hills of northern Italy on Neogene marine deposits and limestone; D, soils of the Po plain and associated hills; E, soils of the central and southern Apennines; F, soils of the mountains of Sardinia and Sicily on magmatic and metamorphic rocks; G, soils of the hills of central and southern Italy on Neogene marine deposits and limestone; H, soils of the hills of central and southern Italy on volcanic deposits and limestone; I, soils of the hills and marine terraces of southern Italy on calcareous sediments; L, soils of the plains and low hills of central and southern Italy. (b) Pie chart shows percentage of the extent of the land use class (A, sector width) and number of rainfall-induced landslides (N_L, sector height) in each land use class. (c) Cumulated event rainfall E (mm) vs. rainfall duration D (h) conditions that have resulted in landslides in A (violet dots), B (light blue dots), C (green dots), E (brown dots), and G (yellow dots). Coloured lines are corresponding 5% thresholds, $T_{5,A}$, $T_{5,B}$, $T_{5,C}$, $T_{5,E}$, and $T_{5,G}$ (Table 1). Data shown in log–log coordinates. (d) $T_{5,A}$, $T_{5,B}$, $T_{5,C}$, $T_{5,E}$, and $T_{5,G}$ thresholds in the range 1 h ≤ D ≤ 120 h, with associated uncertainty portrayed by shaded areas, in linear coordinates. (For interpretation of the references to colour in this figure legend, the reader is referred to the web version of this article.)

undistinguishable, statistically.

4.3. Thresholds for lithological complexes

To study the relationships between rock types and rainfall thresholds, we used a map showing ten lithological complexes, or groups of rock units, in Italy obtained by reclassifying the Geological Map of Italy published by the Italian Istituto Superiore per la Protezione e la Ricerca Ambientale, at 1:500,000 scale (Fig. 6a). In the map showing main lithological complexes, the alluvial deposit complex (AD) covers the largest area (73,631 km^2, 24.5%), followed by the terrigenous (TC, 65,006 km^2, 21.7%), the carbonatic rocks (CC, 54,616 km^2, 18.1%),

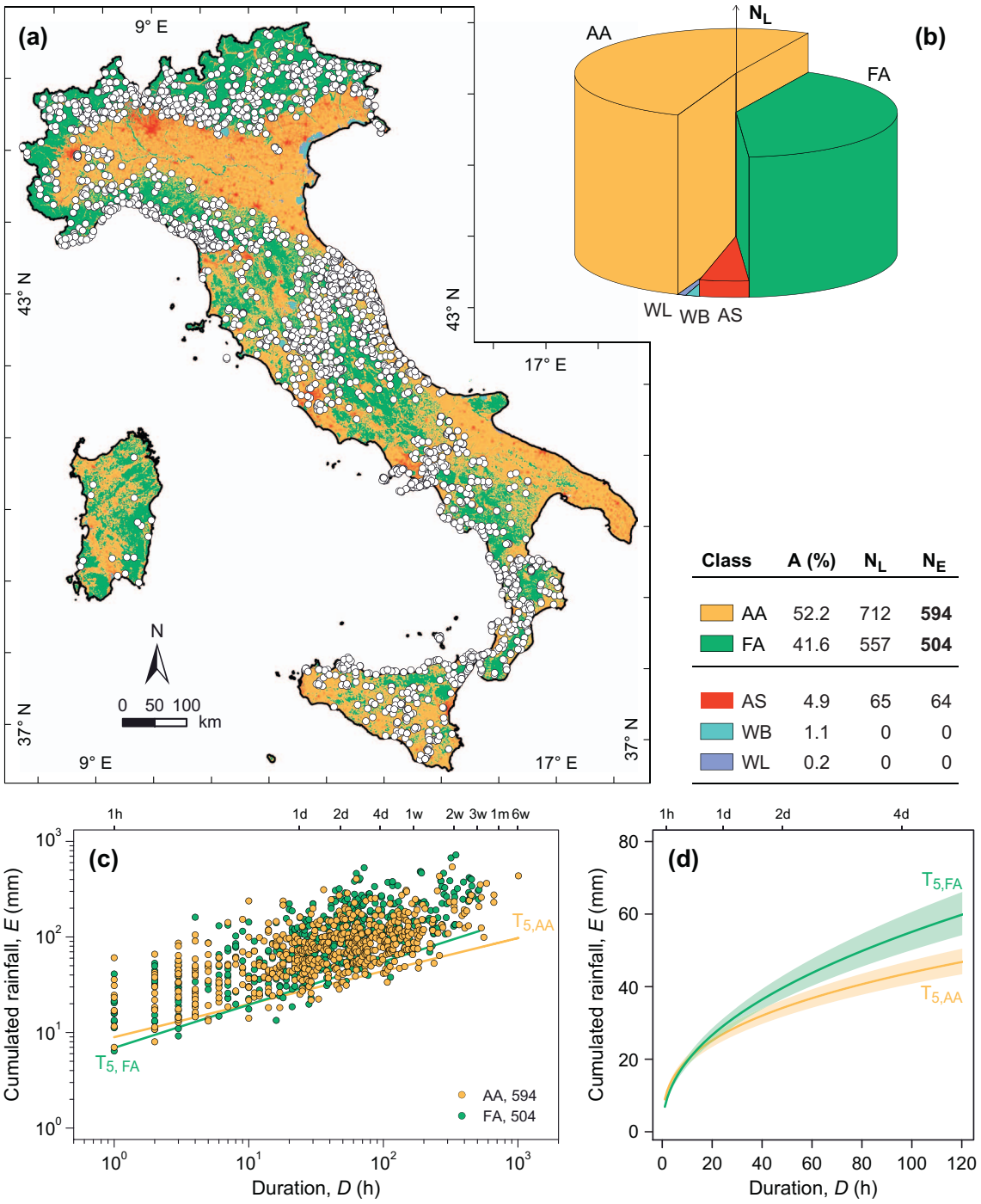

Fig. 8. (a) Map showing a subdivision of Italy in five land cover classes obtained from the first level of the Corine Land Cover (CLC) map released in 2006. Legend: AS, artificial surfaces; AA, agricultural areas; FA, forested and semi-natural areas; WL, wetlands; WB, water bodies. (b) Pie chart shows percentage of the extent of the land cover class (A, sector width) and number of rainfall-induced landslides (N_L, sector height) in each land cover class. (c) Cumulated event rainfall E (mm) vs. rainfall duration D (h) conditions that have resulted in landslides in AA (orange dots) and FA (green dots). Coloured lines are corresponding 5% thresholds, $T_{5,AA}$, $T_{5,FA}$ (Table 1). Data shown in log–log coordinates. (d) $T_{5,AA}$ and $T_{5,FA}$ thresholds in the range 1 h ≤ D ≤ 120 h, with associated uncertainty portrayed by shaded areas, in linear coordinates. (For interpretation of the references to colour in this figure legend, the reader is referred to the web version of this article.)

and the post-orogenic sediments (PO, 48,005 km^2, 15.9%) complexes. The terrigenous complex (TC) has the largest number of landslides (N_L = 668) and of rainfall events with landslides (N_E = 556), followed by the PO (N_L = 498, N_E = 410), and the CC (406, 377) complexes (Fig. 6b). Landslide density is largest in the post-orogenic sediment (PO) and in the terrigenous (TC) complexes ($1.0 \times 10^{-2}\ km^{-2}$), and is similar in the CC, VD, and MC complexes ($0.8 \times 10^{-2}\ km^{-2}$).

Fig. 6c shows, in log-log coordinates, the distribution of the N_E = 1779 (D,E) rainfall conditions responsible for the documented rainfall events with landslides in the six complexes that have $N_E \geq 100$, including TC (N_E = 556 green dots), PO (410 orange dots), CC (377 blue dots), MC (177 purple dots), AD (142 grey dots), and VD (117 brown dots) complexes, with their corresponding 5% ED lithological thresholds, $T_{5,TC}$, $T_{5,PO}$, $T_{5,CC}$, $T_{5,MC}$, $T_{5,AD}$, and $T_{5,VD}$ (Table 1). The thresholds are also shown in Fig. 6d, in linear coordinates and in the range 1 ≤ D ≤ 120 h, with the shaded area depicting the uncertainty associated to the thresholds. Inspection of Fig. 6c, d reveals that, as for the physiographic thresholds, none of the six lithological thresholds can

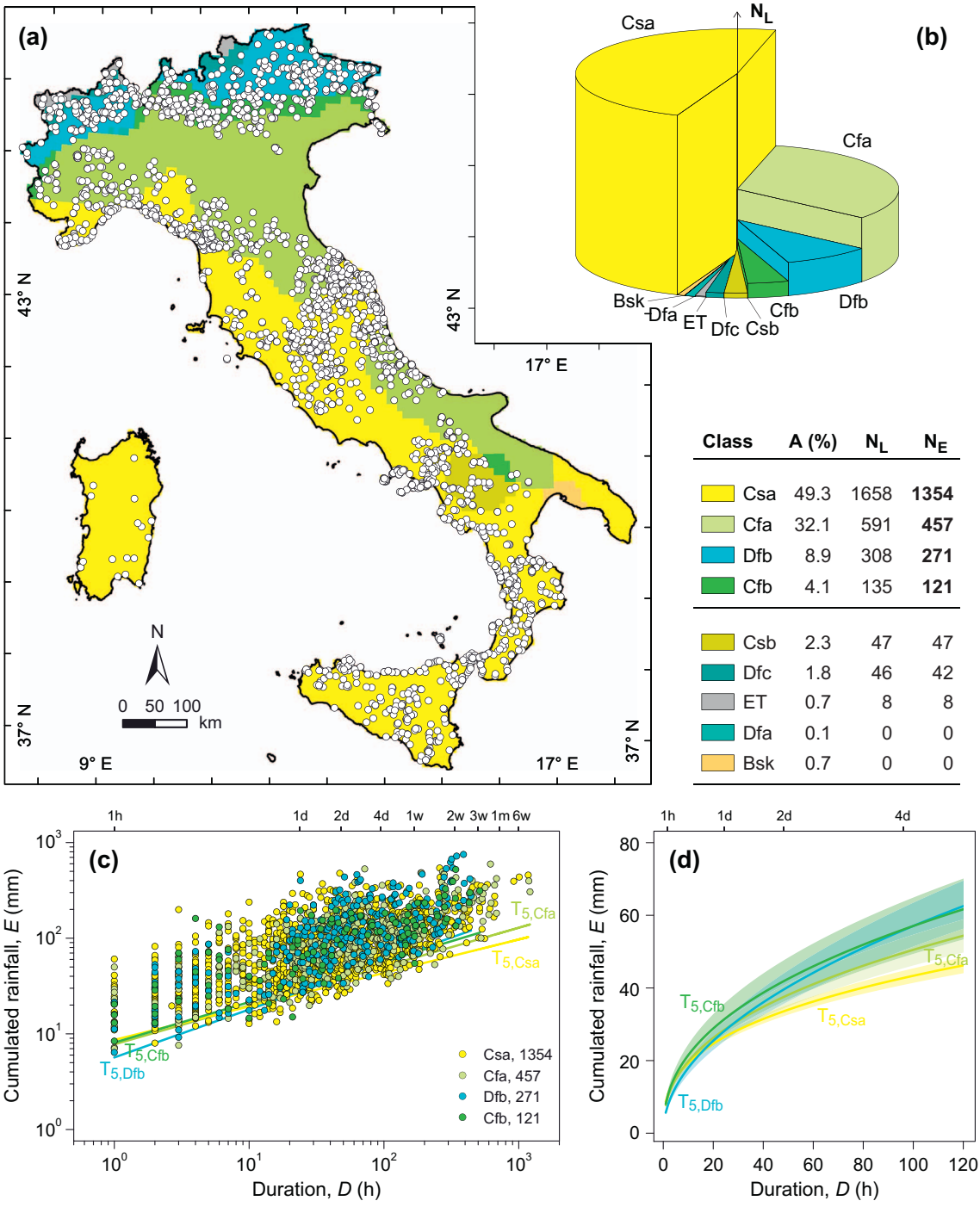

Fig. 9. (a) Map showing a subdivision of Italy into nine climate regions based the World Map of the Koeppen-Geiger climate classification (Peel et al., 2007). Legend: Bsk, arid steppe cold climate; Cfa, temperate climate without dry season and with hot summer; Cfb, temperate climate without dry season and with warm summer; Csa, temperate climate with dry and hot summer; Csb, temperate climate with dry and warm summer; Dfa, cold climate without dry season and with hot summer; Dfb, cold climate without dry season and with warm summer; Dfc, cold climate without dry season and with cold summer; ET, polar climate with tundra. (b) Pie chart shows percentage of the extent of the climate regions (A, sector width) and number of rainfall-induced landslides (N_L, sector height) in each climate region. (c) Cumulated event rainfall E (mm) vs. rainfall duration D (h) conditions that have resulted in landslides in Cfa (light green dots), Cfb (bright green dots), Csa (yellow dots), and Dfb (light blue dots). Coloured lines are corresponding 5% thresholds, $T_{5,Cfa}$, $T_{5,Cfb}$, $T_{5,Csa}$, $T_{5,Dfb}$ (Table 1). Data shown in log–log coordinates. (d) $T_{5,Cfa}$, $T_{5,Cfb}$, $T_{5,Csa}$ and $T_{5,Dfb}$ thresholds in the range 1 h ≤ D ≤ 120 h, with associated uncertainty portrayed by shaded areas, in linear coordinates. (For interpretation of the references to colour in this figure legend, the reader is referred to the web version of this article.)

be separated clearly, for the entire range of the considered rainfall durations. The threshold for the metamorphic rocks ($T_{5,MC}$) is steeper than the other thresholds ($\gamma = 0.51 \pm 0.03$), and the threshold for the post-orogenic sediments ($T_{5,PO}$) is lower that all the other thresholds for $D > 13$ h. The other lithological thresholds ($T_{5,TC}$, $T_{5,CC}$, $T_{5,AD}$, and $T_{5,VD}$) are difficult – or impossible – to separate, statistically.

4.4. Thresholds for soil regions

To explore differences in the rainfall thresholds for different soil regions, we used the pedological map published by Costantini et al. (2012), at 1:1,000,000 scale, who divided Italy in nine soil regions reflecting different morphology, soil water, temperature regime, and soil types, and an additional class including urban areas and water

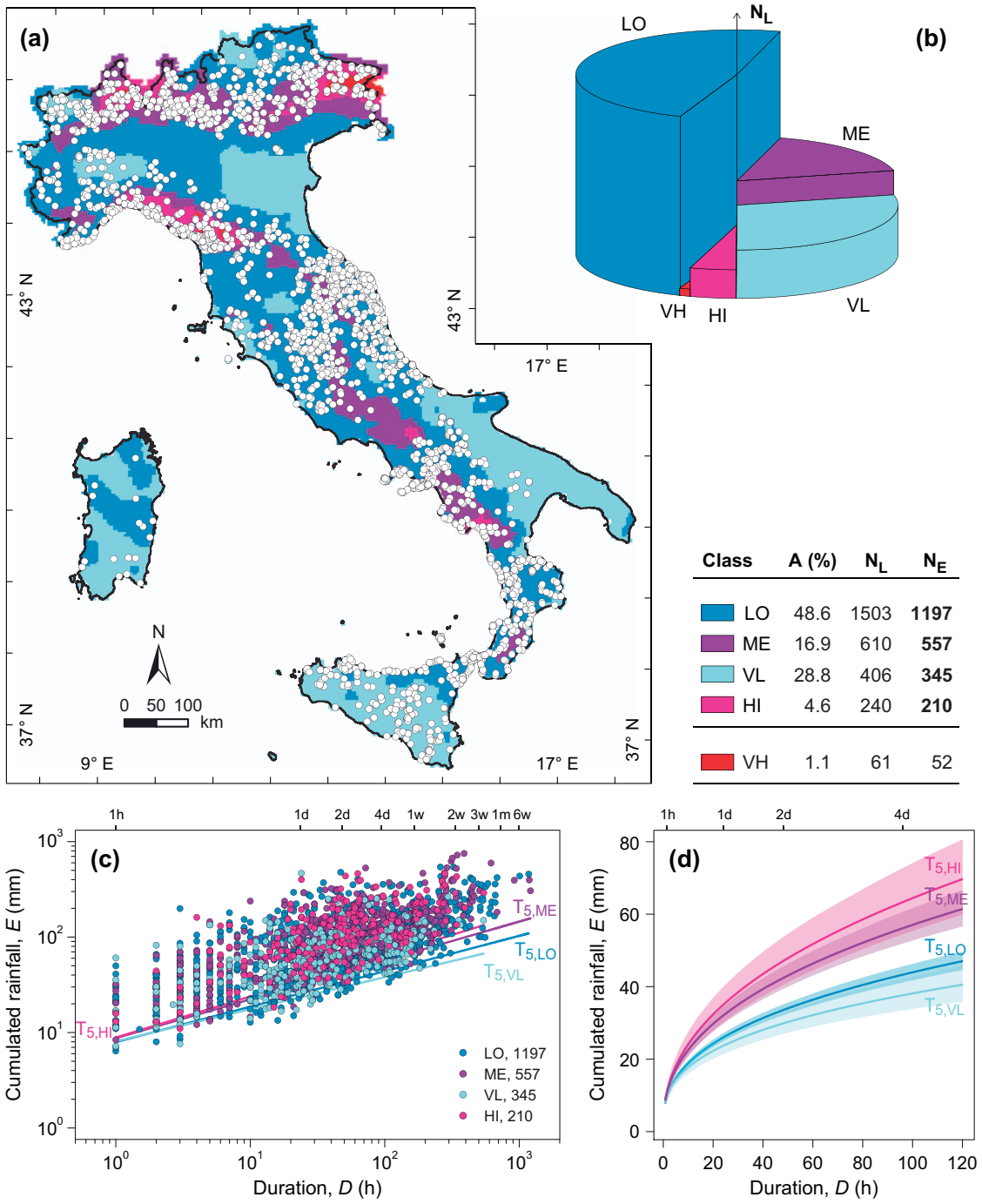

Fig. 10. (a) Map showing a subdivision of Italy into five mean annual precipitation (MAP) classes, modified after Desiato et al. (2014). Legend: VL, very low (MAP ≤ 800 mm); LO, low (800 mm < MAP ≤ 1200 mm); ME, medium (1200 mm < MAP ≤ 1600 mm); HI, high (1600 mm < MAP ≤ 2000 mm); VH, very high (MAP > 2000 mm). (b) Pie chart shows percentage of the extent of the MAP regions (A, sector width) and number of rainfall-induced landslides (N_L, sector height) in each MAP region. (c) Cumulated event rainfall E (mm) vs. rainfall duration D (h) conditions that have resulted in landslides in VL (light blue dots), L (blue dots), M (purple dots), and H (magenta dots). Coloured lines are corresponding 5% thresholds, $T_{5,VL}$, $T_{5,LO}$, $T_{5,ME}$, $T_{5,HI}$ (Table 1). Data shown in log–log coordinates. (d) $T_{5,VL}$, $T_{5,LO}$, $T_{5,ME}$, and $T_{5,HI}$ thresholds in the range 1 h ≤ D ≤ 120 h, with associated uncertainty portrayed by shaded areas, in linear coordinates. (For interpretation of the references to colour in this figure legend, the reader is referred to the web version of this article.)

bodies (U, in this work) (Fig. 7a). Soils in the Alps and the Prealps (A) cover the largest area (50,222 km^2, 16.6%), followed by soils in the Po plain and hills (D, 47,754 km^2, 15.8%), by soils covering hills formed on recent marine sediments in central and southern Italy (G, 47,444 km^2, 15.7%), and soils in the Apennines with a temperate climate (B, 35,107 km^2, 11.7%). Soils in the Alps and the Prealps (A) have the largest number of landslides (N_L = 598) and of rainfall events with landslides (N_E = 534), followed by soils in the hills of central and southern Italy (G, N_L = 579, N_E = 488). Soils in the Po plain (D) have only 39 landslides and 34 landslide events in the catalogue (Fig. 7b). The later was expected, given the flat topography of most of this soil region. Landslide densities in the C, E, B, A, and G soil regions – collectively covering 173,600 km^2, 57.5% of Italy – are all comparable, and in the range from 1.1 × 10^{-2} km^{-2} to 1.3 × 10^{-2} km^{-2}.

Fig. 7c shows the distribution of the N_E = 1697 (D,E) rainfall conditions in the A (534 violet dots), G (488 yellow dots), B (316 light blue dots), E (244 brown dots), and C (115 green dots) soil regions, all having N_E ≥ 100, and their corresponding 5% ED thresholds, $T_{5,A}$, T_{5G},

$T_{5,B}$, $T_{5,E}$, and $T_{5,C}$ (Table 1), which are also shown in Fig. 7d, in linear coordinates, with their estimated uncertainties portrayed by the shaded areas. Inspection of Fig. 7c, d reveals that, considering the uncertainties, also the thresholds for the soil regions cannot be separated, for the entire range of the considered rainfall durations. The $T_{5,C}$ threshold for soils covering the hills of northern Italy is higher than all the other soil thresholds, for $D \leq 48$ h. For longer rainfall durations, the highest threshold is $T_{5,A}$, for soils in the Alps and the Prealps. For $D > 20$ h, the lowest threshold is $T_{5,G}$, for soils covering the hills of central and southern Italy, which is very similar to the $T_{5,E}$, for soils of the central and southern Apennines, and the $T_{5,E}$ threshold is lower than the $T_{5,G}$ threshold for $D \leq 20$ h. We note that the $T_{5,C}$ threshold has the largest uncertainty (the largest shaded area, $\Delta\alpha = 3.2$, $\Delta\gamma = 0.05$), which we attribute to the relatively small number of empirical data points in this soil region ($N_E = 115$).

4.5. Thresholds for land cover types

To study the effects of land cover on rainfall thresholds, we exploited the Coordination of Information on the Environment (CORINE) land cover (CLC) map published in 2006 at 1:100,000 scale, available from www.pcn.minambiente.it. For our analysis, we attributed each rainfall event with landslides in the catalogue to one of five, first-level CLC classes (Fig. 8a). We found that agricultural areas (AA) have the largest extent (157,477 km^2, 52.2%), followed by forested and semi-natural areas (FA, 125,568 km^2, 41.6%), and by artificial surfaces (AS, 14,901 km^2, 4.9%). The AA land cover class has also the largest number of landslides ($N_L = 712$) and of rainfall events with landslides ($N_E = 594$), followed by FA ($N_L = 557$, $N_E = 504$) and AS (65, 64) (Fig. 8b). The remaining land cover classes (WB, WL) did not contain landslides; and this was expected. Interestingly, landslide density is similar in the three land cover classes with landslide events (AS, FA, AA), in the range between 0.4×10^{-2} and 0.5×10^{-2} km^{-2}.

Fig. 8c portrays the distribution of the $N_E = 1098$ (*D*,*E*) rainfall conditions in the AA class (594 orange dots) and in the FA class (504 green dots) that have resulted in landslides, together with the corresponding 5% *ED* thresholds, $T_{5,AA}$ and $T_{5,FA}$ (Table 1). The same two thresholds are shown in Fig. 8d, in linear coordinates and in the range $1 \leq D \leq 120$ h, with their estimated uncertainty depicted by the shaded areas. Inspection of Fig. 8c, d and Table 1 reveals that the two thresholds are quite different, with $T_{5,FA}$ significantly steeper ($\gamma = 0.45 \pm 0.02$) than $T_{5,AA}$ ($\gamma = 0.35 \pm 0.02$). As a result, $T_{5,AA}$ is higher than $T_{5,FA}$ for short rainfall durations ($D \leq 6$ h), and $T_{5,FA}$ is higher than $T_{5,AA}$ for longer rainfall durations ($D > 6$ h); with the two thresholds statistically distinct (i.e., considering their uncertainties) for $D > 42$ h.

4.6. Thresholds for climatic regions

To examine the role of climate on rainfall thresholds, we used the World Map of the Köppen-Geiger climate classification published by Peel et al. (2007) based on 0.5 × 0.5-degree latitude/longitude gridded data. Based on this map, nine climate regions exist in Italy (Fig. 9a). Inspection of the map shows that the temperate climate with dry and hot summers (Csa) predominates, covering 148,977 km^2 (49.3%), followed by the region with temperate climate without dry season and with hot summer (Cfa, 96,690 km^2, 32.1%), and the region with cold climate without dry season and with warm summer (Dfb, 26,818 km^2, 8.9%). The Csa climate region has also the largest number of landslides ($N_L = 1658$) and of rainfall events with landslides ($N_E = 1354$), followed by the Cfa ($N_L = 591$, $N_E = 457$), Dfb (398, 271), and Cfb (135, 121) regions; whereas the Dfa and Bsk regions did not contain landslides in the catalogue (Fig. 9b). Landslide density was largest in the Cfb, Csa and the Dfb climate regions (1.1×10^{-2} km^{-2}), and smallest in the Cfa region (0.6×10^{-2} km^{-2}).

Fig. 9c portrays the $N_E = 2203$ (*D*,*E*) rainfall conditions that have resulted in landslides in the Csa (1354 yellow dots), Cfa (457 light green dots), Dfb (271 cyan dots), and Cfb (121 green dots) climate regions having $N_E \geq 100$, with the corresponding 5% *ED* threshold lines shown by the corresponding coloured lines, $T_{5,Csa}$, $T_{5,Cfa}$, $T_{5,Dfb}$, and $T_{5,Cfb}$ (Table 1). The thresholds are also shown, in linear coordinates and in the range $1 \leq D \leq 120$ h, in Fig. 9d together with their estimated uncertainty (shaded areas). Inspection of Fig. 9c, d reveals that the thresholds determined for the different climate regions are all very similar, with minor differences in the steepness of the curves, which is lowest for $T_{5,Csa}$ ($\gamma = 0.35 \pm 0.01$) and highest for $T_{5,Dfb}$ ($\gamma = 0.50 \pm 0.03$). For $D > 18$ h, the $T_{5,Csa}$ threshold, that predominates in southern Italy, in Sicily and Sardinia, is the lowest of all the climate thresholds.

4.7. Thresholds for precipitation regions

The rainfall regime is known to influence the landslide triggering conditions in Italy (Crosta, 1998; Aleotti, 2004; Guzzetti et al., 2007). For this work, we used the mean annual precipitation (MAP, in mm) as a proxy for the regional rainfall regime, and we investigated the variation of the rainfall thresholds in five different MAP regions, obtained from the work of Desiato et al. (2014). Fig. 10a shows that almost half of Italy is characterized by low values of the MAP (LO, 152,641 km^2, 48.6%), followed by VL (28.8%), ME (16.9%), HI (4.6%), and VH (1.1%). Given the climate conditions in Italy (Fig. 9a), the reduction in size of the precipitation regions with the increasing MAP was expected. Due to its large size, the precipitation region with a low MAP (LO) has the largest number of landslides ($N_L = 1503$) and of rainfall events with landslides ($N_E = 1197$), followed by the ME ($N_L = 610$, $N_E = 557$), VL (406, 345), HI (240, 210), and VH (61, 52) precipitation regions. However, as expected, the largest landslide densities were found in the HI (1.7×10^{-2} km^{-2}) and the VH (2.0×10^{-2} km^{-2}) regions, and the VL region exhibited the lowest landslide density (0.4×10^{-2} km^{-2}).

Fig. 10c portrays the $N_E = 2309$ (*D*,*E*) rainfall conditions that resulted in landslides in the four out of the five precipitation regions with $N_E \geq 100$, namely, LO (1197 blue dots), ME (557 purple dots), VL (345 light blue dots), and HI (210 magenta dots) regions, with the corresponding 5% *ED* thresholds, $T_{5,LO}$, $T_{5,ME}$, $T_{5,VL}$, and $T_{5,HI}$ (Table 1), shown by the coloured lines. The four thresholds are also shown in Fig. 10d, in linear coordinates and in the reduced range $1 \leq D \leq 120$ h, with the shaded areas depicting the uncertainty associated to each threshold. Inspection of Fig. 10d reveals that the four thresholds can be clustered into two groups; a lower group with the $T_{5,VL}$ and $T_{5,LO}$ thresholds, and a higher group with the $T_{5,ME}$ and $T_{5,HI}$ thresholds. We note that the two groups are distinct for all the considered rainfall durations. Further inspection of Fig. 10d and Table 1 reveals that the rainfall thresholds increase in steepness with increasing MAP, going from $\gamma = 0.34 \pm 0.02$ for the VL region to $\gamma = 0.43 \pm 0.03$ for the HI region.

5. Discussion

5.1. Data

Our catalogue of rainfall events with landslides lists events responsible for the first reported slope failure in each of the considered rainfall events. Other landslides occurred, or reported in the same general area after the first failure were not considered. This reduced the number of rainfall events with landslides in the catalogue, and it is different from the approach adopted by other authors who have used all (or most) of the landslide information available to them (e.g., Crosta, 1998; Aleotti, 2004; Guzzetti et al., 2007, 2008; Ponziani et al., 2011; Rosi et al., 2012; Berti et al., 2012; Segoni et al., 2014; Gariano et al., 2015b; Lagomarsino et al., 2015).

Inspection of the catalogue reveals that individual rainfall events

with landslides N_E, have caused from one to eleven landslides, N_L. We searched for a dependency linking N_L to N_E, and found $N_L = 1.2\ N_E$, with the multiplying factor remaining about the same for all the considered environmental subdivisions. The small multiplying factor is due to the fact that for many known landslides insufficient information on their geographical location or the time of the failures was available, and the landslides were not included in the catalogue.

The landslide information used in this work was collected specifically with the aim of defining rainfall thresholds. As a result, 2040 (72.4%) of the landslides in the catalogue have a temporal accuracy better than 6 h (T_1 and T_2 in Fig. 2c), and 2592 (91.9%) landslides are located within a distance of < 1.8 km from the expected exact (and unknown) location of the landslides (P_1 and P_2 in Fig. 2b). We consider this a good result for a national catalogue of rainfall-induced landslides spanning multiple years (19), and listing many rainfall events with landslides. The result was obtained adopting strict criteria for the selection of the rainfall events with landslides. > 40% of the landslides for which information was available were not included in the catalogue because the information was considered insufficient, or inaccurate. This occurred e.g., where (i) the cause of the landslide was unknown, (ii) landslides where not triggered by rainfall, but e.g., by snow melt, earthquake, anthropic actions, (iii) rain gauges were not available near the landslide, (iv) information on the location of the landslide was inaccurate, precluding the identification of a suitable rain gauge to reconstruct the triggering landslide rainfall history, and (v) the time of occurrence of the landslide was not known with at least a daily accuracy.

We stress the importance – and the difficulty – of collecting accurate information on the temporal and geographical location of the landslides. As an example, and remaining in Italy, to investigate the temporal correlation and clustering of landslides in the Emilia-Romagna region, northern Italy, Rossi et al. (2010) and Witt et al. (2010) used an historical catalogue of 2255 landslides between 1951 and 2002, compiled by the Emilia-Romagna Geological Survey (Emilia-Romagna SGSS, 2006). In this vast historical catalogue, only the day of occurrence of the landslides is known. Similarly, Ponziani et al. (2011), to establish rainfall thresholds and for soil moisture modelling in Umbria, central Italy, used an historical catalogue listing an unknown number of landslides between 1989 and 2001. Most of the landslides in the catalogue had a daily temporal accuracy. To study variations in the occurrence of rainfall-induced landslides in Calabria, southern Italy, Gariano et al. (2015b) used a similar historical catalogue listing 7600 landslides between June 1920 and December 2010, with daily temporal accuracy. We emphasize that these catalogues, and other similar regional catalogues, do not contain a sufficient number of landslides with exact, hourly, or sub-daily temporal accuracy (T_1 and T_2) to define accurate rainfall thresholds to be used in landslide early warning systems, adopting the approach discussed in this work.

Our catalogue of rainfall events with landslides covers the 19-year period from January 1996 to February 2014, with the majority of the N_E between 2011 and 2014 (Fig. 2a). This is a short period compared to the periods covered by other landslide catalogues (Reichenbach et al., 1998; Guzzetti et al., 2007, 2008; Polemio and Petrucci, 2010; Ponziani et al., 2011; Berti et al., 2012; Stoffel et al., 2014; Gariano et al., 2015b), or by sets of extreme meteorological events that have resulted in landslides (Crosta, 1998; Aleotti, 2004; Giannecchini et al., 2016), used to establish rainfall thresholds in Italy. The relatively short period considered in our study reduces the uncertainty in the rainfall information associated to rain gauges of different types and technologies, that is known to affect catalogues covering longer periods. The short period also limits the effects of climatic, land-use/land-cover changes, and of other environmental changes that may affect the amount of rainfall necessary to trigger the landslides. We maintain that this is an advantage when defining thresholds for operational landslide forecasting and early warning (Keefer et al., 1987; Tiranti and Rabuffetti, 2010; Rossi et al., 2012; Segoni et al., 2013; Stähli et al., 2015; Piciullo et al., 2016). However, thresholds defined considering a specific climate period may change due to climate and environmental changes, and should be checked and adjusted periodically (Gariano and Guzzetti, 2016).

5.2. Thresholds

Following a consolidated approach (Caine, 1980; Crosta, 1998; Aleotti, 2004; Guzzetti et al., 2007, 2008; Brunetti et al., 2010; Berti et al., 2012; Segoni et al., 2014; Lagomarsino et al., 2015), to determine the rainfall thresholds for the possible occurrence of landslides in Italy, we adopted a power law model. Although other models are available in the literature (e.g., Cannon and Ellen, 1985; Wieczorek, 1987; Cannon, 1988; Corominas and Moya, 1999; Crosta and Frattini, 2001; Zezere and Rodrigues, 2002), the power law model is the most popular (Guzzetti et al., 2007, 2008), most probably because of its simplicity – a threshold is completely defined by only two parameters (α, γ), and because it allows using empirical data for a reduced range of the (D,E) conditions that can result in landslides to define a threshold, maximizing the use of the landslide and rainfall information. A limitation of the self-similar scaling behaviour represented by a power-law model is that the rainfall conditions that can result in landslides scale with the rainfall duration, implying that the physical conditions (e.g., rainfall, infiltration) that control the initiation of landslides also exhibit a self-similar behaviour. Another limitation is that a power law threshold model is apparently independent of any physical (i.e., geological, geomorphological, hydrological) criteria (Reichenbach et al., 1998). However, Alvioli et al. (2014), using a spatially distributed, physically-based slope stability model, have shown that the mean rainfall conditions that can result in slope instabilities in central Italy match well a power law threshold curve, providing evidence for a physical basis for the power law thresholds.

Differently from other consolidated approaches, we have defined cumulated event rainfall–rainfall duration, ED thresholds (Innes, 1983), instead of the most popular rainfall intensity – rainfall duration, ID thresholds (Caine, 1980; Guzzetti et al., 2007, 2008). As discussed in Peruccacci et al. (2012), when determining a functional dependency between two variables, it is assumed that the variables measure independent quantities. This assumption is violated when searching for a relationship between the rainfall duration D, and the rainfall mean intensity I, because the rainfall mean intensity depends on the rainfall duration, through the cumulated rainfall. For this reason, we prefer searching for ED thresholds. We note here that it is trivial to convert an ED threshold to the corresponding ID threshold, considering that $\gamma = -\beta + 1$, where β is the slope of the corresponding ID power law threshold $I = \alpha D^{-\beta}$, with I the mean rainfall intensity (in mm h^{-1}).

Studying the variables controlling the obtained thresholds for Italy and for the different environmental subdivisions (Table 1), the following considerations emerged. First, the parameters α and γ that determine the thresholds are linearly correlated. For larger values of γ (steeper thresholds), the values of α (the intercept) decrease. This was expected, as a steeper threshold results in a lower intercept of the threshold curve. Yet, depending on the distribution of the empirical (D,E) points, two parallel thresholds with the same γ can have different intercept values (e.g., $T_{5,P6}$ and $T_{5,VL}$ in Table 1).

Second, the two measures of uncertainties ($\Delta\alpha$, $\Delta\gamma$) depend on the size of the empirical DE distribution. For a large (small) number of N_E, $\Delta\alpha$ and $\Delta\gamma$ tend to decrease (increase) (Table 1). The uncertainties are also mutually dependent. For large (small) values of $\Delta\gamma$, $\Delta\alpha$ is also large (small). This is evidence that a distribution of empirical (D,E) pairs that results in a large (small) uncertainty in the scaling exponent of the threshold ($\Delta\gamma$), will also result in a large (small) uncertainty in the intercept ($\Delta\alpha$), and vice-versa. Further, $\Delta\gamma$ is not related to γ, whereas $\Delta\alpha$ depends positively on α. In other words, the uncertainty around the scaling exponent of the threshold curve ($\Delta\gamma$) does not depend on the steepness of the curve (γ), whereas the uncertainty on the intercept

($\Delta\alpha$) increases with increasing intercept values (α).

Third, no clear relationship exists between the ranges of the cumulated event rainfall (E_{max}-E_{min}) and of the event rainfall duration (D_{max}-D_{min}), and the parameters controlling the thresholds (γ, α), or their uncertainties ($\Delta\gamma$, $\Delta\alpha$). Lastly, increasing the areal extent (size) of the environmental subdivision, the number of landslides (N_L), and the number of rainfall events with landslides (N_E), also increases. This was expected because given the method adopted to compile the catalogue, a larger area includes more landslides than a smaller area. We further observe that increasing the size of the environmental subdivisions, the uncertainties $\Delta\gamma$ and $\Delta\alpha$ decrease. We explain this with the increasing number of N_E which contributes to reducing the uncertainty.

5.3. Analysis of the thresholds

We defined thresholds for 26 of the 48 (54.2%) environmental subdivisions considered in our work (Table 1). The subdivisions range in size from 10,834 ($T_{5,C}$) to 157,239 ($T_{5,AA}$) km^2, and contain from a minimum of N_E = 115 ($T_{5,C}$) to a maximum of N_E = 1354 ($T_{5,Csa}$) empirical data points. The number of N_E was insufficient to define a threshold for the remaining 22 subdivisions, which range from 231 (Dfa) to 44,754 (D) km^2, and contain from nil to a maximum of N_E = 91 (HI) empirical data points.

Analysis of the 26 thresholds defined for the six environmental zonations of Italy considered in this work (Figs. 5–10) reveals that the thresholds are all similar, and cover a limited portion of the possible, vast *DE* domain (Fig. 11a). We conclude that despite the large environmental (i.e., topographical, lithological, pedological, land use and cover, climatic, meteorological) variability, the rainfall conditions that can result in landslides in Italy do not vary largely.

Inspection of Fig. 11b, where the same 26 thresholds are shown in linear coordinates and for rainfall duration, $D \leq 120$ h, reveals that the thresholds can be loosely clustered into four groups, depending on their higher/lower position in the *DE* plot. The uppermost group (i) consists of the $T_{5,HI}$ threshold defined for the meteorological region HI characterized by a high mean annual precipitation i.e., 1600 < MAP ≤ 2000 mm. This region is present in the central and the eastern Alps, in the eastern Liguria region, in the Apuane Alps (Tuscany), in small parts of the central Apennines, and in the mountains bordering the gulf of Policastro, southern Italy (Fig. 10). In these areas, shallow landslides are frequent and abundant (Marchi et al., 2002; Bacchini and Zannoni, 2003; Guzzetti et al., 2004; Marra et al., 2015; Nikolopoulos et al., 2015; Giannecchini et al., 2016).

The lowest group (iv) comprises three thresholds characterized by less severe rainfall conditions that can initiate landslides, including the $T_{5,PO}$ threshold for post-orogenic sediments (Fig. 6), the $T_{5,P7}$ threshold for the Sicily physiographic province (Fig. 5), and the $T_{5,VL}$ threshold defined for the meteorological region with a MAP ≤ 800 mm (Fig. 10). We observe a clear geographical association between the considered lithological, physiographic, and meteorological variables. Large parts of the Sicily topographic province are underlined by post-orogenic sediments, and exhibit a very low MAP. Similarly, in areas underlined by post-orogenic sediments in central Piedmont, northern Italy, and in central Italy, the MAP is very low. It is therefore expected that the three thresholds $T_{5,PO}$, $T_{5,P7}$ and $T_{5,VL}$ are similar. We further observe that the $T_{5,P7}$ threshold for the Sicily physiographic province is similar to the 5%

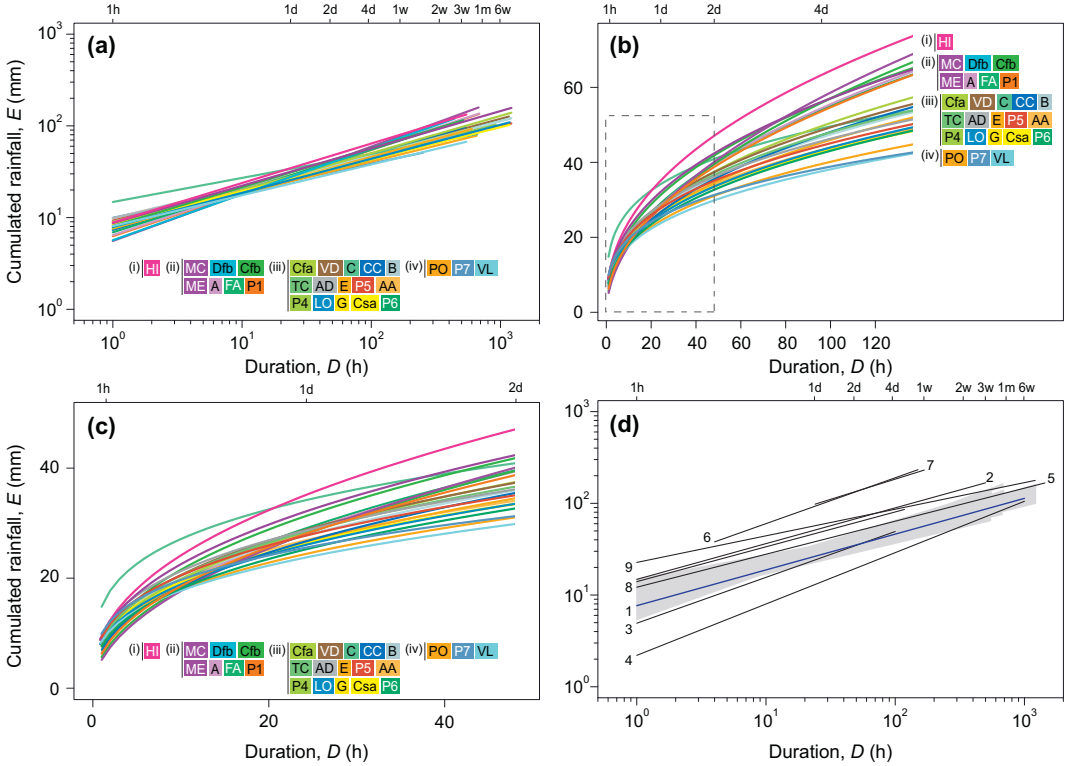

Fig. 11. (a) Cumulated event rainfall–rainfall duration (*ED*) 5% thresholds for possible landslide occurrence for 26 environmental conditions in Italy, in log–log coordinates. Letters in coloured boxes show threshold codes given in Table 1. Roman numbers (i, ii, iii, iv) identify groups of thresholds. (b) The same thresholds shown in (a) in linear coordinates in the range of rainfall duration 1 h < $D \leq 120$ h. Dashed box identifies area shown in (c). (c) The same thresholds shown in (b) in the range of rainfall duration 1 h < $D \leq 48$ h, in linear coordinates. (d) Comparison between the 5% national threshold for Italy, $T_{5,IT}$ (blue line, IT in Table 1) and the range of environmental thresholds (grey shaded area) defined in this work, with global (2–4), national (5), and regional (6–10) thresholds given in the literature (black lines). (For interpretation of the references to colour in this figure legend, the reader is referred to the web version of this article.)

(Source: 1, national threshold for Italy defined in this work (IT in Table 1); 2, Caine (1980); 3, Innes (1983); 4, Guzzetti et al. (2008); 5, Brunetti et al. (2010); 6, Aleotti (2004); 7a, 7b, modified after Tiranti and Rabufetti (2010); 8, modified after Berti et al. (2012); 9, Rosi et al. (2012); 10, modified after Giannecchini et al. (2016). Other thresholds for regions and sites Italy can be found e.g., in Guzzetti et al. (2007, 2008); Brunetti et al. (2010); Martelloni et al. (2012); Peruccacci et al. (2012); Segoni et al. (2014); Vennari et al. (2014); Gariano et al. (2015a); Melillo et al. (2016).)

exceedance probability threshold proposed by Gariano et al. (2015a) and Melillo et al. (2016) for nearly the same geographical area.

The other two groups of thresholds are best separated for rainfall durations exceeding three days, and each encompasses several thresholds (Fig. 11b, Table 1). The upper group (ii) comprises the $T_{5,MC}$, $T_{5,Dfb}$, $T_{5,Cfb}$, $T_{5,ME}$, $T_{5,A}$, $T_{5,FA}$, and $T_{5,P1}$ thresholds, and the lower group (iii) includes the remaining 15 thresholds ($T_{5,Cfa}$, $T_{5,VD}$, $T_{5,C}$, $T_{5,CC}$, $T_{5,B}$, $T_{5,TC}$, $T_{5,AD}$, $T_{5,E}$, $T_{5,P5}$, $T_{5,AA}$, $T_{5,P4}$, $T_{5,LO}$, $T_{5,G}$, $T_{5,Csa}$, $T_{5,P6}$, Fig. 11b). For the thresholds in the upper group (ii), inspection of the environmental maps (Figs. 5–10) also reveals geographical associations between some of the variables, the most evident of which is in the Alpine physiographic region (P1), where metamorphic rocks (MC) are covered by alpine and pre-alpine soils (A), and by forests (FA), in a region where climate is cold (Dfb), and the MAP is medium (ME). We attribute this outcome to the fact that in most of the Alps the considered environmental variables cover approximately the same areas, and therefore the corresponding rainfall thresholds are similar.

Further inspection of Fig. 11b and Table 1, and of Figs. 5–10, allows for the following general considerations. With increasing rock strength, that we infer loosely from the rock types (Fig. 6), the thresholds become higher in the *DE* plot. This indicates that more rainfall is required to trigger landslides in strong rocks than in weak rocks. Indeed, the threshold for post-orogenic sediments (PO) comprising clay, silt, sand, and gravel, is significantly lower than the threshold for the terrigenous complex (TC) comprising massive and layered sandstone and marl in various proportions, which is lower that the threshold for the carbonate rock complex (CC) made up of massive and layered limestone, with limited marl and chert, that in turn is lower than the threshold for metamorphic rocks (MC) that include chiefly hard gneiss and schists. The association between the lithological type (and the inferred rock strength) and the more/less severe rainfall conditions that can result in landslides, was expected.

Similarly, for a given rainfall duration *D*, forests (FA) require larger event cumulated rainfall (higher threshold) than agricultural areas (AA) (lower threshold). This association was also expected. We also find a clear association between the MAP in a meteorological region (Fig. 10) and the position of the corresponding threshold in the *DE* plot. With higher (lower) MAP, the empirical thresholds are also higher (lower). This suggests that the landscape adjusts to the local rainfall conditions and that, other environmental conditions being similar, more rainfall is required to initiate landslides where the MAP is high than where it is low (Wilson, 2000).

Fig. 11c shows the portion of the *DE* domain for $D \leq 48$ h, and $E \leq 52$ mm. In this reduced range, most of the empirical environmental thresholds overlap and intersect, making it difficult (or impossible) to separate them. This has implications for the possible use of the thresholds for operational landslide forecasting in landslide early warning systems (Keefer et al., 1987; Chleborad, 2003; Aleotti, 2004; Godt et al., 2006; Tiranti and Rabuffetti, 2010; Rossi et al., 2012; Segoni et al., 2013; Stähli et al., 2015; Piciullo et al., 2016). Despite the relatively large number of empirical data points ($N_E = 2309$), and the large number of (*D*,*E*) points used to determine each threshold ($N_E > 100$), the differences in the cumulated event rainfall that may result in landslides for $D \leq 24$ h are limited between the thresholds. As an example, the cumulated event rainfall *E*, varies between 5.5 and 14.8 mm for $D = 1$ h, between 13.7 and 23.6 mm for $D = 6$ h, between 19.5 and 28.2 mm for $D = 12$ h, and between 23.9 and 34.9 mm for $D = 24$ h. We conclude that with the available data it is difficult to distinguish between different thresholds for operational purposes (Calvello and Piciullo, 2016; Piciullo et al., 2016).

5.4. Comparison with other thresholds

The grey shaded area in Fig. 11d portrays the range of (*D*,*E*) conditions covered by the ensemble of the 26 thresholds defined in this work for different environmental settings, together with the general (national) threshold for Italy also defined in this work (blue line, $T_{5,IT}$, $E = 7.7 \pm 0.3 \times D^{0.39 \pm 0.01}$). Not surprisingly, the $T_{5,IT}$ threshold falls well within the range of rainfall conditions identified by the other environmental thresholds. The $T_{5,IT}$ national threshold is significantly lower than the global threshold proposed by Caine (1980) (2 in Fig. 11d), significantly higher than the global threshold proposed by Innes (1983) (3), and much higher than the global threshold proposed by Guzzetti et al. (2008) (4); the later particularly for $D \leq 24$ h.

The $T_{5,IT}$ national threshold is also significantly lower than the similar national threshold proposed by Brunetti et al. (2010) ($E = 12.2 \pm 0.65 \times D^{0.36 \pm 0.01}$) who used the same statistical approach adopted in this work, and an historical catalogue of 753 rainfall events with landslides in Italy in the 169-year period 1841–2009. We attribute the difference between the two national thresholds to (i) the different methods used to collect the rainfall and the landslide information, (ii) the different periods covered by the catalogues (19 vs. 169 years), and (iii) the larger size of the new catalogue. About 80% of the landslides in the catalogue of Brunetti et al. (2010) were obtained from the scientific literature, which mainly provides information on severe rainfall events that have resulted in abundant landslides, biasing the threshold towards higher values. Conversely, the catalogue used in this work was compiled using chiefly regional and local newspapers, and reports of the local fire brigades that include information on low to moderate rainfall events that have triggered single or few landslides. In addition, about 75% of the events considered by Brunetti et al. (2010) were located in northern Italy, chiefly in the Alps, where rainfall thresholds are higher, as confirmed by our results (Fig. 11b). Overall, we maintain that the difference between our new national threshold $T_{5,IT}$, and the threshold proposed by Brunetti et al. (2010) measures the difference in the quality of the landslide information, and to the more systematic approach used to identify the rainfall conditions responsible for the landslides (Peruccacci et al., 2012).

For further comparison, Fig. 11d shows a selection of rainfall thresholds for possible landslide occurrence proposed in the literature for different areas in Italy, including the Piedmont region, NW Italy (6, Aleotti, 2004; 7a and 7b, Tiranti and Rabuffetti, 2010), the Emilia-Romagna region, northern Apennines (8, Berti et al., 2012), Tuscany, central Italy (9, Rosi et al., 2012), and the Apuane Alps, NW Tuscany (10, Giannecchini et al., 2016). Comparison of these regional and local thresholds with our environmental thresholds is difficult and uncertain, because the thresholds taken from the literature were defined using different methods and techniques, different landslide and rainfall information and, most importantly, adopting different criteria to identify the rainfall events with landslides, and consequently the rainfall conditions that have resulted in landslides (Melillo et al., 2015, 2016).

Despite the uncertainty, we note that our new environmental thresholds are much lower than the threshold proposed by Aleotti (2004) for the Piedmont region, NW Italy (6), by Tiranti and Rabuffetti (2010) for the mountain (7a) and for the hilly (7b) parts of the Piedmont region, and by Berti et al. (2012) for the Emilia-Romagna region (8); are lower than the threshold proposed by Giannecchini et al. (2016) for the Apuane Alps (10); and that the threshold proposed by Rosi et al. (2012) for Tuscany (9) lays near the upper boundary of the range of rainfall conditions identified by the ensemble of thresholds as possible triggers of rainfall-induced landslides (grey area in Fig. 11d).

The threshold of Aleotti (2004) for the Piedmont region corresponds to an exceedance probability of 10%, higher than the 5% exceedance probability adopted in this work, and was obtained analysing landslides triggered by five severe meteorological events in 1994, 1996 and 2000. This explains why the threshold is higher than the $T_{5,IT}$. For their "pragmatic thresholds" for mountains and hills in the Piedmont region, Tiranti and Rabuffetti (2010) used information from 10 severe rainfall events that triggered many landslides between 1992 and 2002. Use of information from severe events explains why these thresholds are much higher than our national threshold. We also note that their threshold for

the mountains (7a in Fig. 11d) is significantly higher than our threshold for the Alpine physiographic region (P1), and their threshold for the hills (7b in Fig. 11d) is significantly higher than our thresholds for post orogenic sediments ($T_{5,PO}$) and for soils mantling hilly terrains in northern Italy ($T_{5,C}$).

To determine rainfall thresholds for the Emilia-Romagna region, Berti et al. (2012) exploited a regional catalogue of 1168 historical landslides in the period 1939–2000, in the range of triggering rainfall $1 < D \leq 32$ day, for which the date of occurrence was known with daily accuracy. In the same geographical region, our catalogue lists 51 rainfall events with landslides in the period 2003–2010, in the range $3 < D \leq 303$ h, most of which with 6-hour accuracy. We further note that the 5% threshold proposed by Berti et al. (2012) requires a daily cumulated rainfall of 100 mm, which is much higher than what we find in our catalogue. We maintain that the significant difference between the two 5% thresholds depends on the type of the landslide catalogues, the accuracy of the landslide occurrence time, and the method used to reconstruct the rainfall events responsible for the landslides.

Giannecchini et al. (2016) studied the rainfall conditions responsible for debris flows involving quarry waste from marble caves in a 100 km^2 area in the Apuane Alps, between 1950 and 2005. We explain the difference between the thresholds with the small size of the study area (Guzzetti et al., 2007), and the materials involved in the debris flows, which are coarse and highly permeable, and require larger amounts of rainfall to fail.

5.5. Application of the thresholds for landslide early warning

A thorough examination of the possible use of our new national threshold $T_{5,IT}$, and of the environmental thresholds (Table 1, Fig. 11), for operational landslide forecasting in Italy is beyond the scope of this work. However, three considerations are possible.

First, thresholds for operational landslide forecasting should be constructed using information on landslides typical of the geographical area or region where the early warning system operates. Also, the thresholds should be constructed using information that includes, as much as possible, all the rainfall events that have resulted in landslides in an area, and not only the extreme or the most severe events, as this will result in high or very high thresholds that (i) may miss a number of landslides triggered less severe rainfall events, and (ii) may not be particularly useful for regional or national operational landslide forecasting. For this reason, we consider our national $T_{5,IT}$ threshold better suited than the national threshold for Italy proposed by Brunetti et al. (2010), because the $T_{5,IT}$ threshold was constructed considering less severe rainfall events that have resulted in landslides.

Second, despite the significant amount of landslide and rainfall information available for this work, the number of N_E was insufficient to determine accurate thresholds for 22 environmental subdivisions (45.8%, Table 1). Excluding the subdivisions where landslide susceptibility is expected to be very low (e.g., P2, AD, D), we consider this a result of the strict criteria adopted to select (or exclude) a landslide to reconstruct a N_E. Also, despite the fact that the uncertainty ($\Delta\alpha$, $\Delta\gamma$) associated to a threshold, and the variation of the threshold around the central tendency line decrease with the increasing number of N_E, for several thresholds the uncertainty remains large, $\Delta\alpha > 1.0$ and $\Delta\gamma \geq 0.03$ ($T_{5,C}$, $T_{5,MC}$, $T_{5,VD}$, $T_{5,P7}$, $T_{5,HI}$, $T_{5,Cfb}$). This is partly a consequence of the internal variability of the environmental subdivisions. We conclude that the definition of accurate rainfall thresholds for small geographical areas, or for specific environmental conditions, remains difficult. This has an impact on the application of the thresholds in early warning systems. We maintain that accurate thresholds defined for larger areas and characterized by a low uncertainty are preferable to thresholds defined for smaller areas but affected by a higher uncertainty. The inherent variability of the landslide types and of the conditions that favour landslides in large areas should be considered when transforming the thresholds in related landslide warning levels (Calvello et al., 2015; Calvello and Piciullo, 2016; Piciullo et al., 2016).

Lastly, we note that the red points shown in Fig. 4a, representing 52 rainfall events that have resulted in 55 landslides with casualties in the 19-year period 1996–2014 in Italy, are all located well above the new national $T_{5,IT}$ threshold, and have a lower boundary well represented by a 20% exceedance probability threshold line. We conclude that a $T_{20,IT}$ threshold could be adopted to forecast fatal rainfall-induced landslides in Italy.

6. Conclusions

Using accurate landslide and rainfall information, we built a catalogue of 2309 rainfall events with – mostly shallow – landslides in Italy from January 1996 to February 2014. To reconstruct the rainfall history presumably responsible for each landslide, we adopted criteria that considered the distance and position of the landslides and the rain gauges, and the accuracy of the information on the time of occurrence of each landslide. The result is the single largest and more accurate collection of information on rainfall events with landslides in Italy compiled specifically to determine rainfall thresholds for possible landslide occurrence.

Adopting a consolidated approach (Brunetti et al., 2010; Peruccacci et al., 2012; Vennari et al., 2014; Gariano et al., 2015a), we defined empirical cumulated event rainfall–rainfall duration, *ED* power law thresholds for Italy, and for 26 environmental subdivisions of Italy, and we used the thresholds to confront the rainfall conditions that can result in rainfall-induced landslides in different environmental settings in Italy. Analysis of the thresholds (Table 1) revealed that the parameters controlling the power law thresholds (α, the intercept, and γ, the exponent) are correlated, with steeper (less steep) thresholds exhibiting smaller (larger) intercepts. The uncertainties associated to the thresholds ($\Delta\alpha$, $\Delta\gamma$) are also dependent, with large (small) values of $\Delta\gamma$, corresponding to large (small) values of $\Delta\alpha$, and both reducing with an increasing number of rainfall events with landslides, N_E.

We found that despite the large environmental variability, the rainfall conditions that can result in landslides do not differ much in Italy (Fig. 11a). The finding encourages the use of empirical rainfall thresholds for operational landslide forecasting. On the other hand, the result, and the considerable size of the catalogue of rainfall events with landslides ($N_E = 2309$) built for this work, pose an empirical limitation to the possibility to define accurate thresholds for small geographical areas. We conclude that the definition of accurate rainfall thresholds for small geographical areas (local thresholds), or for specific environmental conditions, is difficult (or even impossible) with the criteria adopted in this work. This has implications for the use of the rainfall thresholds for local operational landslide forecasting (Piciullo et al., 2016). However, we observe that the 52 rainfall events that have resulted in landslides with casualties between 1996 and 2014 in Italy, are predicted by a 20% exceedance probability threshold. We conclude that a $T_{20,IT}$ threshold could be adopted to forecast fatal rainfall-induced landslides in Italy.

Detailed analysis of the environmental thresholds allowed identifying a few significant differences between the thresholds (Table 1). Of the several subdivisions used, only the geographical distribution of the mean annual precipitation (MAP, Desiato et al., 2014) (Fig. 10), a proxy for the regional rainfall regime, resulted in a clear separation of the thresholds, with threshold curves becoming higher and steeper for a larger MAP. We consider the fact that more rainfall is required to initiate landslides where the MAP is larger than where it is smaller, evidence that the landscape adjusts to the rainfall conditions. The fact that the MAP – a proxy for meteorology – was more distinctive than the other environmental conditions (e.g., topography, lithology, land cover), should not be surprising, as rainfall, the sole trigger of the landslides considered in this study, depends directly on meteorology.

We further observed that with increasing rock strength, inferred

from the rock types, the thresholds become higher and steeper. This empirical evidence confirms that more rainfall is required to trigger landslides in strong rocks than in weak rocks; and it was expected. Similarly, areas covered by forests exhibit a higher threshold than agricultural areas, indicating that forested areas need more rainfall than agricultural areas to initiate landslides; and it was also expected. Finally, we found distinct geographical associations between some of the considered environmental conditions that are reflected in the rainfall thresholds, which are similar. As an example, the threshold for the Alpine physiographic region is nearly identical to the threshold defined for the alpine and pre-alpine soils region, and similar to the threshold defined for areas with a cold climate.

We maintain that our findings foster the understanding of the rainfall conditions that can result in rainfall-induced landslides in Italy, and their variations in different environmental settings. We expect that the method adopted in this work to define and compare the thresholds, will have an impact on the definition of new rainfall thresholds for the possible occurrence of rainfall-induced landslides in Italy, and elsewhere.

Acknowledgments

Work financially supported by the Italian National Department for Civil Protection (DPC) (Intese Operative DPC n. 619, 672, 1015, 1181; Accordi di Collaborazione 2014, 2015, 2016), that also provided access to the national rainfall database for the period 2002–2014. Loredana Antronico, Devis Bartolini, Andrea Deganutti, Giulio Iovine, Silvia Luciani, Fabio Luino, Michela Rosa Palladino, Mario Parise, Oreste Terranova, Laura Turconi, Carmela Vennari, Giovanna Vessia, and Alessia Viero (CNR IRPI) contributed to collect landslide information, and to reconstruct rainfall events with landslides. We are grateful to Ivan Marchesini (CNR IRPI) who contributed to the organization of the rainfall information used in this work, to Mauro Cardinali (CNR IRPI) for discussing the lithological classification of Italy, and to Paola Salvati (CNR IRPI) who provided information on landslides with human consequences in Italy. Stefano Luigi Gariano and Massimo Melillo were supported by DPC grants.

References

Aleotti, P., 2004. A warning system for rainfall-induced shallow failures. Eng. Geol. 73, 247–265. http://dx.doi.org/10.1016/j.enggeo.2004.01.007.

Alvioli, M., Guzzetti, F., Rossi, M., 2014. Scaling properties of rainfall induced landslides predicted by a physically based model. Geomorphology 213, 38–47. http://dx.doi.org/10.1016/j.geomorph.2013.12.039.

Ardizzone, F., Basile, G., Cardinali, M., Casagli, N., Del Conte, S., Del Ventisette, C., Fiorucci, F., Garfagnoli, F., Gigli, G., Guzzetti, F., Iovine, G., Mondini, A.C., Moretti, S., Panebianco, M., Raspini, F., Reichenbach, P., Rossi, M., Tanteri, L., Terranova, O.G., 2012. Landslide inventory map for the Briga and the Giampilieri catchments, NE Sicily, Italy. J. Maps 8 (2), 176–180. http://dx.doi.org/10.1080/17445647.2012.694271.

Bacchini, M., Zannoni, A., 2003. Relations between rainfall and triggering of debris-flow: a case study of Cancia (Dolomites, Northeastern Italy). Nat. Hazards Earth Syst. Sci. 3, 71–79. http://dx.doi.org/10.5194/nhess-3-71-2003.

Berti, M., Martina, M.L.V., Franceschini, S., Pignone, S., Simoni, A., Pizziolo, M., 2012. Probabilistic rainfall thresholds for landslide occurrence using a Bayesian approach. J. Geophys. Res. 117, F04006. http://dx.doi.org/10.1029/2012JF002367.

Bivand, R.S., Gebhardt, A., 2000. Implementing functions for spatial statistical analysis using the R language. J. Geogr. Syst. 2, 307–317. http://dx.doi.org/10.1007/PL00011460.

Borrelli, L., Cofone, G., Coscarelli, R., Gullà, G., 2015. Shallow landslides triggered by consecutive rainfall events at Catanzaro strait (Calabria–Southern Italy). J. Maps 11 (5), 730–744. http://dx.doi.org/10.1080/17445647.2014.943814.

Brunetti, M.T., Peruccacci, S., Rossi, M., Luciani, S., Valigi, D., Guzzetti, F., 2010. Rainfall thresholds for the possible occurrence of landslides in Italy. Nat. Hazards Earth Syst. Sci. 10, 447–458. http://dx.doi.org/10.5194/nhess-10-447-2010.

Caine, N., 1980. The rainfall intensity-duration control of shallow landslides and debris flows. Geografiska Annaler A 62, 23–27. http://dx.doi.org/10.2307/520449.

Calcaterra, D., Parise, M., Palma, B., 2003. Combining historical and geological data for the assessment of the landslide hazard: a case study from Campania, Italy. Nat. Hazards Earth Syst. Sci. 3 (1/2), 3–16. http://dx.doi.org/10.5194/nhess-3-3-2003.

Calvello, M., Piciullo, L., 2016. Assessing the performance of regional landslide early warning models: the EDuMaP method. Nat. Hazards Earth Syst. Sci. 16, 103–122. http://dx.doi.org/10.5194/nhess-16-103-2016.

Calvello, M., Neiva d'Orsi, R., Piciullo, L., Paes, N., Magalhaes, M., Alvarenga Lacerda, W., 2015. The Rio de Janeiro early warning system for rainfall-induced landslides: analysis of performance for the years 2010–2013. Int. J. Disaster Risk Reduct. 12, 3–15. http://dx.doi.org/10.1016/j.ijdrr.2014.10.005.

Cannon, S.H., 1988. Regional rainfall-threshold conditions for abundant debris-flow activity. In: Ellen, S.D., Wieczorek, G.F. (Eds.), Landslides, Floods, and Marine Effects of the Storm of January 3–5, 1982, in the San Francisco Bay Region, California. U.S. Geological Survey Professional Paper 1434. pp. 35–42.

Cannon, S.H., Ellen, S.D., 1985. Rainfall conditions for abundant debris avalanches, San Francisco Bay region, California. Calif. Geol. 38, 267–272.

Cardinali, M., Galli, M., Guzzetti, F., Ardizzone, F., Reichenbach, P., Bartoccini, P., 2006. Rainfall induced landslides in December 2004 in South-Western Umbria, central Italy: types, extent, damage and risk assessment. Nat. Hazards Earth Syst. Sci. 6, 237–260. http://dx.doi.org/10.5194/nhess-6-237-2006.

Chleborad, A.F., 2003. Preliminary evaluation of a precipitation threshold for anticipating the occurrence of landslides in the Seattle, Washington, Area. US Geological Survey Open-File Report 03–463.

Corominas, J., Moya, J., 1999. Reconstructing recent landslide activity in relation to rainfall in the Llobregat River basin, Eastern Pyrenees, Spain. Geomorphology 30, 79–93. http://dx.doi.org/10.1016/s0169-555x(99)00046-x.

Costantini, E.A.C., L'Abate, G., Barbetti, R., Fantappiè, M., Lorenzetti, R., Magini, S., 2012. Soil map of Italy. Consiglio per la Ricerca e la Sperimentazione in Agricoltura, S.EL.CA Pub., Florence, Italy scale 1:1,000,000.

Crosta, G.B., 1998. Regionalization of rainfall thresholds: an aid to landslide hazard evaluation. Environ. Geol. 35 (2–3), 131–145. http://dx.doi.org/10.1007/s002540050300.

Crosta, G.B., Frattini, P., 2001. Rainfall thresholds for triggering soil slips and debris flow. In: Mugnai, A., Guzzetti, F., Roth, G. (Eds.), Proceedings 2nd EGS Plinius Conference on Mediterranean Storms. Siena, Italy, pp. 463–487.

Desiato, F., Fioravanti, G., Fraschetti, P., Perconti, W., Piervitali, E., 2014. Valori climatici normali di temperatura e precipitazione in Italia. ISPRA, Stato dell'Ambiente 55/2014, ISBN 978-88-448-0689-7, (in Italian).

Emilia-Romagna SGSS (Servizio Geologico, Sismico e dei Suoli), 2006. Geological and Soil Maps of the Emilia-Romagna Region. Historical Landslide Database. http://ambiente.regione.emilia-romagna.it/geologia-en/temi/dissesto-idrogeologico/larchivio-storico-dei-movimenti-franosi [22 December 2016].

Gariano, S.L., Guzzetti, F., 2016. Landslides in a changing climate. Earth Sci. Rev. 162, 227–252. http://dx.doi.org/10.1016/j.earscirev.2016.08.011.

Gariano, S.L., Brunetti, M.T., Iovine, G., Melillo, M., Peruccacci, S., Terranova, O., Vennari, C., Guzzetti, F., 2015a. Calibration and validation of rainfall thresholds for shallow landslide forecasting in Sicily, southern Italy. Geomorphology 228, 653–665 (doi:1016/j.geomorph.2014.10.019).

Gariano, S.L., Petrucci, O., Guzzetti, F., 2015b. Changes in the occurrence of rainfall-induced landslides in Calabria, southern Italy, in the 20th century. Nat. Hazards Earth Syst. Sci. 15, 2313–2330. http://dx.doi.org/10.5194/nhess-15-2313-2015.

Giannecchini, R., Galanti, Y., D'Amato Avanzi, G., Barsanti, M., 2016. Probabilistic rainfall thresholds for triggering debris flows in a human-modified landscape. Geomorphology 257, 94–107. http://dx.doi.org/10.1016/j.geomorph.2015.12.012.

Godt, J.W., Baum, R.L., Chleborad, A.F., 2006. Rainfall characteristics for shallow landsliding in Seattle, Washington, USA. Earth Surf. Process. Landf. 31, 97–110. http://dx.doi.org/10.1002/esp.1237.

Guzzetti, F., 2000. Landslide fatalities and the evaluation of landslide risk in Italy. Eng. Geol. 58, 89–107. http://dx.doi.org/10.1016/S0013-7952(00)00047-8.

Guzzetti, F., Reichenbach, P., 1994. Towards a definition of topographic divisions for Italy. Geomorphology 11 (1), 57–74. http://dx.doi.org/10.1016/0169-555x(94)90042-6.

Guzzetti, F., Tonelli, G., 2004. Information system on hydrological and geomorphological catastrophes in Italy (SICI): a tool for managing landslide and flood hazards. Nat. Hazards Earth Syst. Sci. 4, 213–232. http://dx.doi.org/10.5194/nhess-4-213-2004.

Guzzetti, F., Cardinali, M., Reichenbach, P., 1994. The AVI project: a bibliographical and archive inventory of landslides and floods in Italy. Environ. Manag. 18, 623–633. http://dx.doi.org/10.1007/bf02400865.

Guzzetti, F., Cardinali, M., Reichenbach, P., Cipolla, F., Sebastiani, C., Galli, M., Salvati, P., 2004. Landslides triggered by the 23 November 2000 rainfall event in the Imperia Province, Western Liguria, Italy. Eng. Geol. 73 (3–4), 229–245. http://dx.doi.org/10.1016/j.enggeo.2004.01.006.

Guzzetti, F., Peruccacci, S., Rossi, M., Stark, C.P., 2007. Rainfall thresholds for the initiation of landslides in central and southern Europe. Meteorog. Atmos. Phys. 98, 239–267. http://dx.doi.org/10.1007/s00703-007-0262-7.

Guzzetti, F., Peruccacci, S., Rossi, M., Stark, C.P., 2008. The rainfall intensity-duration control of shallow landslides and debris flow: an update. Landslides 5 (1), 3–17. http://dx.doi.org/10.1007/s10346-007-0112-1.

Innes, J.L., 1983. Debris flows. Prog. Phys. Geogr. 7, 469–501. http://dx.doi.org/10.1177/030913338300700401.

Keefer, D.K., Wilson, R.C., Mark, R.K., Brabb, E.E., Brown, W.M.-I.I.I., Ellen, S.D., Harp, E.L., Wieczorek, G.F., Alger, C.S., Zatkin, R.S., 1987. Real-time landslide warning during heavy rainfall. Science 238, 921–925. http://dx.doi.org/10.1126/science.238.4829.921.

Lagomarsino, D., Segoni, S., Rosi, A., Rossi, G., Battistini, A., Catani, F., Casagli, N., 2015. Quantitative comparison between two different methodologies to define rainfall thresholds for landslide forecasting. Nat. Hazards Earth Syst. Sci. 15, 2413–2423. http://dx.doi.org/10.5194/nhess-15-2413-2015.

Marchi, L., Arattano, M., Deganutti, A.M., 2002. Ten years of debris-flow monitoring in the Moscardo torrent (Italian Alps). Geomorphology 46, 1–17. http://dx.doi.org/10.1016/s0169-555x(01)00162-3.

Marra, F., Nikolopoulos, E.I., Creutin, J.D., Borga, M., 2015. Space-time organization of debris flows-triggering rainfall and its effect on the identification of the rainfall threshold relationship. J. Hydrol. 541, 246–255. http://dx.doi.org/10.1016/j.jhydrol.2015.10.010.

Martelloni, G., Segoni, S., Fanti, R., Catani, F., 2012. Rainfall thresholds for the forecasting of landslide occurrence at regional scale. Landslides 9, 485–495. http://dx.doi.org/10.1007/s10346-011-0308-2.

Melillo, M., Brunetti, M.T., Peruccacci, S., Gariano, S.L., Guzzetti, F., 2015. An algorithm for the objective reconstruction of rainfall events responsible for landslides. Landslides 12 (2), 311–320. http://dx.doi.org/10.1007/s10346-014-0471-3.

Melillo, M., Brunetti, M.T., Peruccacci, S., Gariano, S.L., Guzzetti, F., 2016. Rainfall thresholds for the possible landslide occurrence in Sicily (Southern Italy) based on the automatic reconstruction of rainfall events. Landslides 13 (1), 165–172. http://dx.doi.org/10.1007/s10346-015-0630-1.

Napolitano, E., Fusco, F., Baum, R.L., Godt, J.W., De Vita, P., 2016. Effect of antecedenthydrological conditions on rainfall triggering of debris flows in ash-fall pyroclastic mantled slopes of Campania (southern Italy). Landslides 13, 967–983. http://dx.doi.org/10.1007/s10346-015-0647-5.

Nikolopoulos, E.I., Borga, M., Marra, F., Crema, S., Marchi, L., 2015. Debris flows in the Eastern Italian Alps: seasonality and atmospheric circulation patterns. Nat. Hazards Earth Syst. Sci. 15, 647–656. http://dx.doi.org/10.5194/nhess-15-647-205.

Peel, M.C., Finlayson, B.L., McMahon, T.A., 2007. Updated world map of the Köppen-Geiger climate classification. Hydrol. Earth Syst. Sci. 11, 1633–1644. http://dx.doi.org/10.5194/hessd-4-439-2007.

Peres, D.J., Cancelliere, A., 2014. Derivation and evaluation of landslide-triggering thresholds by a Monte Carlo approach. Hydrol. Earth Syst. Sci. 18, 4913–4931. http://dx.doi.org/10.5194/hess-18-4913-2014.

Peruccacci, S., Brunetti, M.T., Luciani, S., Vennari, C., Guzzetti, F., 2012. Lithological and seasonal control of rainfall thresholds for the possible initiation of landslides in central Italy. Geomorphology 139-140, 79–90. http://dx.doi.org/10.1016/j.geomorph.2011.10.005.

Piciullo, L., Gariano, S.L., Melillo, M., Brunetti, M.T., Peruccacci, S., Guzzetti, F., Calvello, M., 2016. Definition and performance of a threshold-based regional early warning model for rainfall-induced landslides. Landslides. http://dx.doi.org/10.1007/s10346-016-0750-2.

Polemio, M., Petrucci, O., 2010. Occurrence of landslide events and the role of climate in the twentieth century in Calabria, southern Italy. Q. J. Eng. Geol. Hydrogeol. 43, 403–415. http://dx.doi.org/10.1144/1470-9236/09-006.

Ponziani, F., Pandolfo, C., Stelluti, M., Berni, N., Brocca, L., Moramarco, T., 2011. Assessment of rainfall thresholds and soil moisture modeling for operational hydrogeological risk prevention in the Umbria region (central Italy). Landslides 9 (2), 229–237. http://dx.doi.org/10.1007/s10346-011-0287-3.

Reichenbach, P., Cardinali, M., De Vita, P., Guzzetti, F., 1998. Regional hydrological thresholds for landslides and floods in the Tiber River Basin (Central Italy). Environ. Geol. 35 (2–3), 146–159. http://dx.doi.org/10.1007/s002540050301.

Rosi, A., Segoni, S., Catani, F., Casagli, N., 2012. Statistical and environmental analyses for the definition of a regional rainfall threshold system for landslide triggering in Tuscany (Italy). J. Geogr. Sci. 22 (4), 617–629. http://dx.doi.org/10.1007/s11442-012-0951-0.

Rossi, M., Witt, A., Guzzetti, F., Malamud, B.D., Peruccacci, S., 2010. Analysis of historical landslide time series in the Emilia-Romagna region, northern Italy. Earth Surf. Process. Landf. 35 (1123–1137), 2010. http://dx.doi.org/10.1002/esp.1858.

Rossi, M., Peruccacci, S., Brunetti, M.T., Marchesini, I., Luciani, S., Ardizzone, F., Balducci, V., Bianchi, C., Cardinali, M., Fiorucci, F., Mondini, A.C., Reichenbach, P., Salvati, P., Santangelo, M., Bartolini, D., Gariano, S.L., Palladino, M., Vessia, G., Viero, A., Antronico, L., Borselli, L., Deganutti, A.M., Iovine, G., Luino, F., Parise, M., Polemio, M., Guzzetti, F., 2012. SANF: national warning system for rainfall-induced landslides in Italy. In: Eberhardt, E., Froese, C., Turner, A.K., Leroueil, S. (Eds.), Landslides and Engineered Slopes: Protecting Society Through Improved Understanding. Taylor & Francis Group, London, 978-0-415-62123-6, pp. 1895–1899.

Salvati, P., Bianchi, C., Fiorucci, F., Giostrella, P., Marchesini, I., Guzzetti, F., 2014. Perception of flood and landslide risk in Italy: a preliminary analysis. Nat. Hazards Earth Syst. Sci. 14, 2589–2603. http://dx.doi.org/10.5194/nhess-14-2589-2014.

Salvati, P., Rossi, M., Bianchi, C., Guzzetti, F., 2016. Landslide risk to the population of Italy and its geographical and temporal variations. In: Chavez, M., Ghil, M., Urrutia-Fucugauchi, J. (Eds.), Extreme Events: Observations, Modeling, and Economics, Geophysical Monograph 214, first ed. John Wiley & Sons, Inc., pp. 177–194. http://dx.doi.org/10.1002/9781119157052.ch14.

Segoni, S., Rosi, A., Battistini, A., Rossi, G., Catani, F., 2013. A regional real time landslide warning system based on spatially variable rainfall thresholds. Landslide Science and Practice 4, 271–275. http://dx.doi.org/10.1007/978-3-642-31337-0_35.

Segoni, S., Rosi, A., Rossi, G., Catani, F., Casagli, N., 2014. Analysing the relationship between rainfalls and landslides to define a mosaic of triggering thresholds for regional scale warning systems. Nat. Hazards Earth Syst. Sci. 14, 2637–2648. http://dx.doi.org/10.5194/nhess-14-2637-2014.

Stähli, M., Sättele, M., Huggel, C., McArdell, B.W., Lehmann, P., Van Herwijnen, A., Berne, A., Schleiss, M., Ferrari, A., Kos, A., Or, D., Springman, S.M., 2015. Monitoring and prediction in early warning systems for rapid mass movements. Nat. Hazards Earth Syst. Sci. 15 (4), 905–917. http://dx.doi.org/10.5194/nhess-15-905-2015.

Stoffel, M., Tiranti, D., Huggel, C., 2014. Climate change impacts on mass movements – case studies from the European Alps. Sci. Total Environ. 493, 1255–1266. http://dx.doi.org/10.1016/j.scitotenv.2014.02.102.

Terranova, O.G., Gariano, S.L., Iaquinta, P., Iovine, G., 2015. ^{GA}*SAKe*: forecasting landslide activations by a genetic-algorithms-based hydrological model. Geosci. Model Dev. 8, 1955–1978. http://dx.doi.org/10.5194/gmd-8-1955-2015.

Tiranti, D., Rabuffetti, D., 2010. Estimation of rainfall thresholds triggering shallow landslides for an operational warning system implementation. Landslides 7 (4), 471–481. http://dx.doi.org/10.1007/s10346-010-0198-8.

Trigila, A., Iadanza, C., Spizzichino, D., 2010. Quality assessment of the Italian landslide inventory using GIS processing. Landslides 7 (4), 455–470. http://dx.doi.org/10.1007/s10346-010-0213-0.

Trigila, A., Iadanza, C., Bussettini, M., Lastoria, B., Barbano, A., 2015. Dissesto idrogeologico in Italia: pericolosità e indicatori di rischio. Rapporto 2015. Istituto Superiore per la Protezione e la Ricerca Ambientale – ISPRA, Rapporti 233/2015 162 pp. in Italian.

Vennari, C., Gariano, S.L., Antronico, L., Brunetti, M.T., Iovine, G., Peruccacci, S., Terranova, O., Guzzetti, F., 2014. Rainfall thresholds for shallow landslide occurrence in Calabria, southern Italy. Nat. Hazards Earth Syst. Sci. 14, 317–330. http://dx.doi.org/10.5194/nhess-14-317-2014.

Wieczorek, G.F., 1987. Effect of rainfall intensity and duration on debris flows in central Santa Cruz Mountains. In: Costa, J.E., Wieczorek, G.F. (Eds.), Debris Flow-Avalanches: Process, Recognition, and Mitigation. Geological Society of America, Reviews Eng. Geol. 7. pp. 93–104.

Wilson, R.C., 2000. Climatic variations in rainfall thresholds for debris-flows activity. In: Claps, P., Siccardi, F. (Eds.), Proceedings 1st EGS Plinius Conference on Mediterranean Storms. Maratea, pp. 415–424.

Witt, A., Malamud, B.D., Rossi, M., Guzzetti, F., Peruccacci, S., 2010. Temporal correlations and clustering of landslides. Earth Surf. Process. Landf. 35 (10), 1138–1156. http://dx.doi.org/10.1002/esp.1998.

Zezere, J.L., Rodrigues, M.L., 2002. Rainfall thresholds for landsliding in Lisbon Area (Portugal). In: Rybar, J., Stemberk, J., Wagner, P. (Eds.), Landslides. A.A. Balkema, Lisse, pp. 333–338.